A Volcano Rekindled: The Renewed Eruption of Mount St. Helens, 2004–2006
Edited by David R. Sherrod, William E. Scott, and Peter H. Stauffer
U.S. Geological Survey Professional Paper 1750, 2008

Chapter 18

Radar Interferometry Observations of Surface Displacements During Pre- and Coeruptive Periods at Mount St. Helens, Washington, 1992–2005

By Michael P. Poland[1] and Zhong Lu[2]

Abstract

We analyzed hundreds of interferograms of Mount St. Helens produced from radar images acquired by the ERS-1/2, ENVISAT, and RADARSAT satellites during the 1992–2004 preeruptive and 2004–2005 coeruptive periods for signs of deformation associated with magmatic activity at depth. Individual interferograms were often contaminated by atmospheric delay anomalies; therefore, we employed stacking to amplify any deformation patterns that might exist while minimizing random noise. Preeruptive interferograms show no signs of volcanowide deformation between 1992 and the onset of eruptive activity in 2004. Several patches of subsidence in the 1980 debris-avalanche deposit were identified, however, and are thought to be caused by viscoelastic relaxation of loosely consolidated substrate, consolidation of water-saturated sediment, or melting of buried ice. Coeruptive interferometric stacks are dominated by atmospheric noise, probably because individual interferograms span only short time intervals in 2004 and 2005. Nevertheless, we are confident that at least one of the seven coeruptive stacks we constructed is reliable at about the 1-cm level. This stack suggests deflation of Mount St. Helens driven by contraction of a source beneath the volcano.

Introduction

Continuous Global Positioning System (GPS) measurements at Mount St. Helens have provided unequivocal evidence of coeruptive deflation that started in 2004, coincident with the onset of seismicity in late September of that year (Lisowski and others, this volume, chap. 15). These data have been used to model an ellipsoidal source of volume loss between 6 and 12 km depth beneath the volcano (Lisowski and others, this volume, chap. 15; Mastin and others, this volume, chap. 22). In addition, GPS results from in and around the crater, including single-frequency instruments deployed on the growing lava dome, have recorded surface displacements associated with dome extrusion (LaHusen and others, this volume, chap. 16). Interferometric synthetic aperture radar (InSAR) data provide an excellent complement to these GPS data. Though lacking the high temporal resolution of continuous GPS or tiltmeter data, InSAR has the potential to provide much greater spatial resolution of deformation, which is useful both for identifying localized deformation sources and modeling complex source geometries. Further, radar images of Mount St. Helens are available from 1992 onward, making it possible to quantify surface displacements during the 1992–2004 preeruption period, when few other geodetic measurements were collected.

Although InSAR characterizations of surface deformation at shield volcanoes (for example, Amelung and others, 2000a) and calderas (for example, Hooper and others, 2004; Wicks and others, 1998; Wicks and others, 2006) have been quite successful, studies of stratovolcanoes have proven more challenging. This is largely due to the fact that most stratovolcanoes are steep sided and covered to varying degrees by vegetation, snow, and ice, leading to a loss of coherent interferometric signal on and around the volcano, especially for C-band radar wavelengths (Zebker and others, 2000; Lu and others, 2005b; Moran and others, 2006). The great height of many stratovolcanoes, relative to the surrounding terrain, can also create atmospheric conditions that introduce significant artifacts into InSAR results (Beaudecel and others, 2000; Wadge and others, 2006). The combined effects of these conditions prevented the use of coeruptive InSAR data for the analysis of deformation at numerous stratovolcanoes, includ-

[1] U.S. Geological Survey, PO Box 51, Hawaii National Park, HI 96718

[2] U.S. Geological Survey, 1300 SE Cardinal Court, Vancouver, WA 98683

ing Galeras, Colombia; Rincon de la Vieja, Costa Rica; Unzen, Japan; and Merapi, Indonesia (Zebker and others, 2000). Even when coeruptive data for a stratovolcano are coherent, there is no guarantee that deformation will be observed, as demonstrated by results from Fuego and Pacaya, Guatemala; Popocatepetl, Mexico; Sakurajima, Japan (Zebker and others, 2000); Irruputuncu (Zebker and others, 2000; Pritchard and Simons, 2004b) and Lascar (Pritchard and Simons, 2002; Pritchard and Simons, 2004a), Chile; and Shishaldin (Moran and others, 2006), Pavlof, Cleveland, and Korovin, Alaska (Lu and others, 2003b). Lu and others (2003b) and Moran and others (2006) suggested that, at least in the case of Shishaldin, the lack of observed line-of-sight displacements in coeruptive InSAR data may be caused by (1) posteruption motion that balanced preeruption displacements, resulting in no net deformation across the time spanned by the interferograms, (2) the occurrence of deformation in "blind zones" where InSAR data are not coherent, or (3) the lack of any significant deformation associated with the eruption. Pritchard and Simons (2004a; 2004b) suggest similar reasons for the lack of observed deformation in InSAR data from Cerro Irruputuncu and Volcán Lascar, two volcanoes in Chile, in addition to the possibility that the magma reservoir may be too deep to produce surface displacements detectable by InSAR.

Poor coherence at a volcano does not necessarily imply that surface displacements cannot be observed by InSAR. Cerro Hudson is a 10-km-diameter, ice-filled caldera in southern Chile. Despite a complete lack of coherence within and limited coherence outside the caldera, displacements were of sufficient magnitude (15-cm line-of-sight inflation over 3 years) to be detected and distinguished from atmospheric noise (Pritchard and Simons, 2004b). Although large displacements were not observed in individual coeruptive interferograms of Soufrière Hills volcano[1], Montserrat, Wadge and others (2006) identified deformation caused by a variety of processes once they stacked (averaged) multiple interferograms. At stratovolcanoes where coherence is excellent, InSAR studies have resulted in important discoveries of aseismic magma accumulation, including Peulik, Alaska (Lu and others, 2002b) and South Sister, Oregon (Dzurisin and others, 2006; Wicks and others, 2002). In addition, InSAR has been critical for characterizing deformation at many composite volcanoes that have experienced unrest or eruptions, including Westdahl (Lu and others, 2003a), Makushin (Lu and others, 2002a), Akutan (Lu and others, 2000; Lu and others, 2005b), Augustine (Masterlark and others, 2006), and Seguam (Masterlark and Lu, 2004), Alaska; Gada 'Ale, Ethiopia (Amelung and others, 2000b); and several volcanoes in the central and southern Andes (Pritchard and Simons, 2002; 2004a; 2004b). Clearly, the potential for advancing the understanding of pre- and coeruptive activity at Mount St. Helens through InSAR studies is substantial.

We completed an exhaustive analysis of InSAR data collected from Mount St. Helens between 1992 and 2005 from a variety of satellites, ground tracks, time spans, and satellite viewing geometries. Our goals were to (1) obtain high-spatial-resolution coeruptive surface displacement data of the known volcanowide deflation (Lisowski and others, this volume, chap. 15) for input into deformation source models, (2) identify any localized displacements that might not be detectable by GPS or other terrestrial measurements, and (3) identify any displacements precursory to the onset of eruptive activity in 2004. Coherence was poor and atmospheric artifacts were significant in most interferograms; nevertheless, we recognized localized displacements unrelated to volcanic activity and modeled coeruptive subsidence (although poor coherence prevented the use of complex model geometries). Preeruptive interferograms showed no evidence of precursory deformation; however, displacements localized within the crater cannot be ruled out, owing to poor coherence and atmospheric distortions.

Methodology

Traditional InSAR studies combine two radar images of the same area on the ground acquired at different times from nearly the same point in space to determine the deformation over the time spanned along the radar's line-of-sight (LOS). This procedure, unfortunately, does not produce satisfactory results at Mount St. Helens for three reasons: (1) atmospheric path delays, which often correlate with topography, can introduce artifacts that amount to several centimeters of apparent LOS displacement (fig. 1), (2) interferograms that include scenes acquired during nonsummer months are generally incoherent due to seasonal snow cover, and (3) coherence breaks down quickly over time, causing interferograms that span more than one or two years to be mostly incoherent. In fact, in interferograms spanning several months or more, coherence was generally maintained only on deposits that were emplaced during the explosive eruptions of 1980 (for example, May 18, May 25, June 12, July 22), especially north of the volcano and in the upper North Fork Toutle River. As a result, we relied on interferometric stacks to study deformation of Mount St. Helens.

Stacking is a procedure that adds the LOS displacements from multiple interferograms (which may or may not be overlapping in time) acquired along the same look angle. Dividing the summed displacements by the cumulative time spanned results in an average displacement rate (for example, Fialko and Simons, 2001; Peltzer and others, 2001). The technique decreases the magnitude of random noise (primarily atmospheric artifacts) by $N/u^{0.5}$, where N is the error in a single interferogram and u is the number of interferograms in the stack (Bevington and Robinson, 1992, p. 39–40). For

[1] Capitalization of "Volcano" indicates adoption of the word as part of the formal geographic name by the host country, as listed in the Geographic Names Information System, a database maintained by the U.S. Board on Geographic Names. Noncapitalized "volcano" is applied informally—eds.

example, if atmospheric variations typically result in an error of 10 mm/yr, a stack of 25 interferograms would reduce the noise level to about 2 mm/yr (assuming atmospheric path delay errors have similar magnitudes in all interferograms). In contrast, signals that persist over time—including steady deformation due to volcanic or tectonic activity—are emphasized because the signal is manifested in all interferograms in the stack. InSAR stacks have been able to distinguish displacement rates as low as a few millimeters per year (Wright and others, 2001, 2004) but are useful only when the strength and geometry of the deformation source do not vary significantly over time, meaning that nonlinear deformation rates or changes in source location or geometry are not easily recovered in interferometric stacks.

We do not expect changes in source geometry over time to bias the interferometric stacks. The geometry of the magmatic system of Mount St. Helens has been investigated using both petrologic (for example, Rutherford and others, 1985; Cashman, 1988; Cashman, 1992; Pallister and others, 1992) and seismic (Scandone and Malone, 1985; Barker and Malone, 1991; Lees, 1992; Moran, 1994; Musumeci and others, 2002) techniques and includes a reservoir at around 6–10 km depth connected to the surface by a near-vertical conduit. The conduit appears to have been sealed at a depth of about 2 km following the end of the 1980–86 eruptive period (Moran, 1994). Any pre- or coeruptive deformation associated with unrest beginning in 2004 will likely have a source within this system (especially at the levels around the 6–10-km-depth reservoir or 2-km-depth seal).

Similarly, deformation rates during both the pre- and coeruptive periods appear to be approximately linear, so time-variable displacements will not bias deformation rates derived by stacking. Electronic Distance Measurement (EDM) and campaign GPS measurements in the inter-eruptive period, from late 1986 through the first half of 2004, indicate that little deformation occurred, especially after 1991 (Lisowski and others, this volume, chap. 15). In addition, individual interferograms that span time periods before

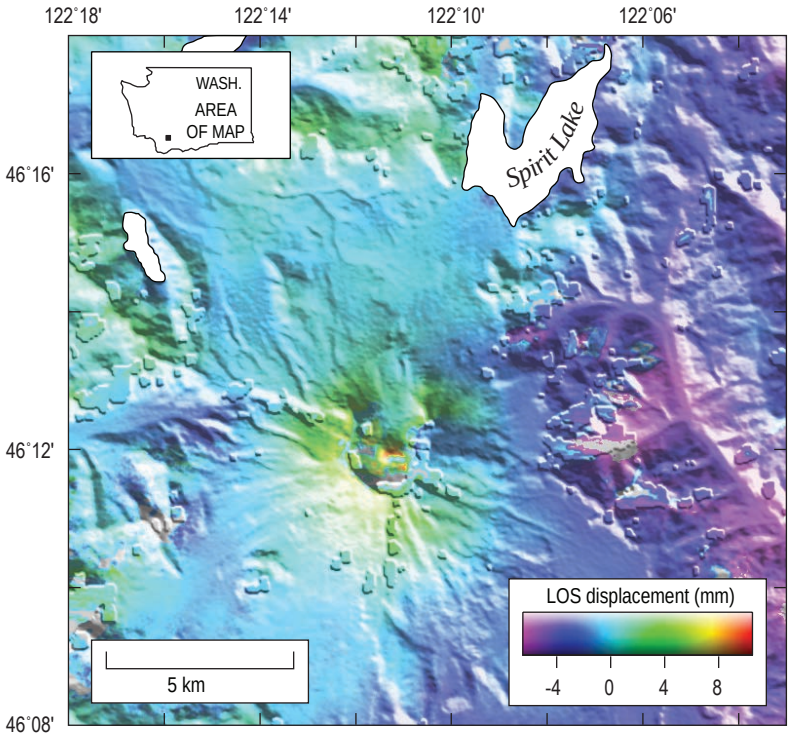

Figure 1. Interferogram of Mount St. Helens, Washington, formed from ERS-1 orbit 21415 (August 19, 1995) and ERS-2 orbit 2243 (September 24, 1995). Interferogram spans only 36 days during summer months, hence high level of coherence. Phase correlates strongly with topography, so Mount St. Helens shows apparent line-of-sight (LOS) lengthening, while lower valleys to east show LOS shortening. Such behavior is characteristic of strong atmospheric influence. Topographic irregularities caused by areas of no data in SRTM DEM.

the start of the unrest in September 2004 show no unambiguous signs of volcanowide deformation. If preeruptive surface displacements occurred, the motion must therefore have been small in magnitude but may have accumulated over time. Coeruptive displacements, measured by continuous GPS starting on September 23, 2004, are generally linear after the first few weeks of the activity (Lisowski and others, this volume, chap. 15) and suggest only minor temporal or spatial variations in the contraction of a source at depth beneath Mount St. Helens.

An unusually large InSAR data set, summarized in table 1, is available for Mount St. Helens, including multiple satellites with a variety of imaging geometries. For preeruptive time periods, we analyzed data from ERS-1, ERS-2, and ENVISAT. Usable data from the first two satellites span 1992–2001 and are available for four orbital tracks, whereas a sufficiently large archive of ENVISAT data is available from one track to allow an assessment of the surface displacement field in 2003–4. Our coeruptive InSAR data set includes five ENVISAT and two RADARSAT tracks. All possible interferograms from each independent track with perpendicular baselines of less than 300 m were created.

Topographic corrections to interferograms utilized the 30-m resolution Shuttle Radar Topography Mission (SRTM) digital elevation model (DEM), which was generated in 2000 (Farr and Kobrick, 2000). The older National Elevation Dataset (NED) 30-m DEM, created before 1986, contains fewer holes than the SRTM data, but its use resulted in deformation artifacts in interferograms in the area of Mount St. Helens crater. Significant topographic changes have occurred in the crater since the end of the 1980–86 eruptive period, most notably the growth of a glacier that had reached a maximum thickness of 200 m by the time eruptive activity resumed in 2004 (Schilling and others, 2004; Walder and others, this volume, chap. 13). The more recent SRTM DEM accounts for growth of the glacier and other changes since 1986 and does not introduce significant artifacts related to topographic change. Interferograms were smoothed using the filtering strategy of Goldstein and Werner (1998) and unwrapped following Chen and Zebker (2001).

From this collection of interferograms, we omitted all images that spanned less than 100 days (except for coeruptive ENVISAT mode 2, track 385, where the only interferograms with perpendicular baselines less than 300 m spanned 70 days or less), because images that span such short times have a low signal-to-noise ratio given the low displacement rates known from GPS (Lisowski and others, this volume, chap. 15). There is no upper limit on the time spanned, although interferograms that showed no or very limited coherence, including nearly all images that span more than two years, were omitted from the analysis. Stacks of each independent track were computed from this modified data set, and only pixels that are coherent in 60 percent of the input images are included in the final stack. Five preeruption and seven coeruption stacks were created, with 3 to 38 input interferograms each (table 1).

Preeruptive Stacks

Results

In preeruptive stacks (figs. 2–6), the range of displacements for each track is generally small, suggesting that the random atmospheric signal has been mostly removed. The lack of significant topography-correlated phase at Mount Adams (which we assume to be undeforming, based on the absence of other signs of unrest) in tracks that both cover and are coherent around both volcanoes (figs. 4, 5) further supports our assertion that atmospheric noise has been mostly suppressed by stacking.

None of the preeruption stacks show any signs of volcanowide deformation, suggesting that no significant surface displacements accumulated over the times spanned by the stacks. Unfortunately there are no InSAR results available between late 2001 and early 2003, so we cannot rule out deformation during this time period. No volcanowide displacements are apparent in the one stack that covers the early 2003 to September 2004 epoch (up to the start of the eruption), suggesting that no centimeter-level displacements on the flanks of the volcano occurred in the months immediately preceding the start of the eruption.

Despite this lack of signal, the five preeruption stacks do reveal at least three localized areas of surface displacement that are unrelated to the magmatic system of Mount St. Helens. All three regions are patches of subsidence located on the May 18, 1980, debris-avalanche deposit (fig. 2). The area with the highest subsidence rate, as much as 15 mm/yr (LOS), is directly north of the crater (site 1 in fig. 2), near the base of Johnston Ridge, and had been recognized previously in individual interferograms by Diefenbach and Poland (2003). A second, less distinct area located near the outlet of Coldwater Lake (site 2 in fig. 2) is subsiding at a rate of slightly less than 5 mm/yr (LOS). The third patch of subsidence, which is sinking at an LOS rate of approximately 6 mm/yr, is in the North Fork Toutle River valley, just southeast of Elk Rock and immediately upstream from a valley constriction (site 3 in fig. 2). The latter two patches had not been recognized previously.

The stacks presented in figures 2 through 6 give average deformation rates. To assess whether or not the subsidence rates of the three localized patches changed during 1992–2005, we used the individual unwrapped interferograms to reconstruct the temporal evolution of the deformation following the method of Berardino and others (2002). At Mount St. Helens, all five preeruption stacks suggest a constant subsidence rate of the area near the base of Johnston Ridge (fig. 7*A*). The four ERS-1/2 tracks are directly comparable in these time series, because they have similar look angles (table 1), and we assume that the deformation is dominated by vertical motion. In addition, the ENVISAT mode 2, track 156, time series confirms that the subsidence was continuing at least into 2004 at a similar rate. Subsidence near the mouth of Coldwater Lake (fig. 7*B*) and below Elk Rock (fig. 7*C*) may have decayed

Table 1. Characteristics of SAR data from Mount St. Helens, Washington, used in stacks and corresponding figures.

[Mode not shown for ERS-1/2 satellite data, which have only one mode. RADARSAT does not use track numbers. A, ascending; D, descending. Incidence angle is measured in degrees from vertical. Number of interferograms (igrams) indicates those used to construct the stack. Figure numbers correspond to this chapter.]

Satellite	Mode	Track	A or D	Incidence angle (deg)	Years spanned	Number of igrams	Figure No.
Preeruptive SAR data							
ERS-1/2	-	156	D	23.2	1992–2001	36	2
ERS-1/2	-	163	A	23.2	1993–2000	7	3
ERS-1/2	-	385	D	23.2	1992–2001	38	4
ERS-1/2	-	392	A	23.2	1995–2000	7	5
ENVISAT	IS 2	156	D	22.8	2003–2004	6	6
Coeruptive SAR data							
ENVISAT	IS 2	156	D	22.8	2004–2005	7	8
ENVISAT	IS 2	163	A	22.8	2004–2005	13	9
ENVISAT	IS 2	385	D	22.8	2004–2005	3[1]	10
ENVISAT	IS 2	392	A	22.8	2004–2005	6	11
ENVISAT	IS 6	20	A	40.9	2004–2005	13	12
RADARSAT	S 2	-	A	27.6	2004–2005	9	13
RADARSAT	S 5	-	A	39.1	2004–2005	6	14

[1] Note that all three input interferograms span 70 days or less.

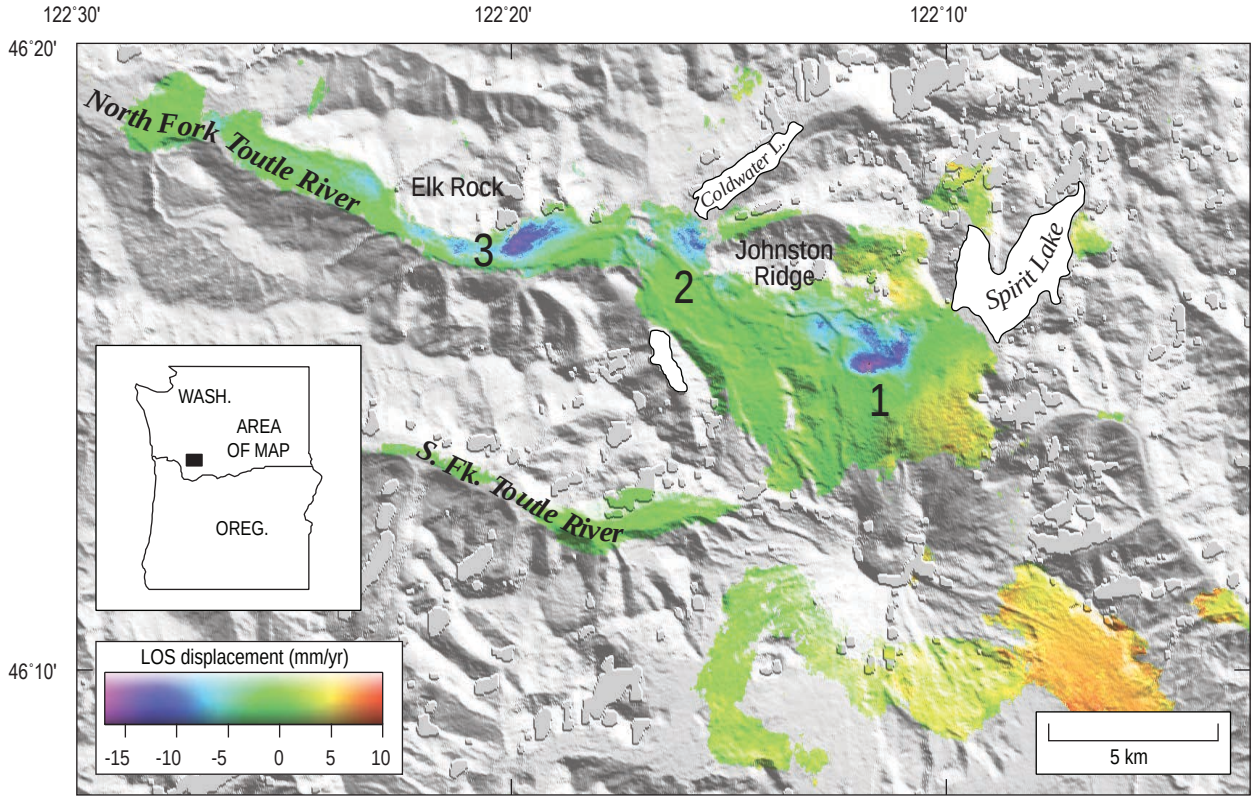

Figure 2. ERS-1/2, track 156, interferometric stack of Mount St. Helens, Washington, composed of 36 interferograms spanning preeruptive 1992–2001 period. Inset shows location of stack. Locations of major features referred to in the text are labeled. Image shows three areas of subsidence in debris-avalanche deposit—1 (Johnston Ridge), 2 (Coldwater), and 3 (Elk Rock).

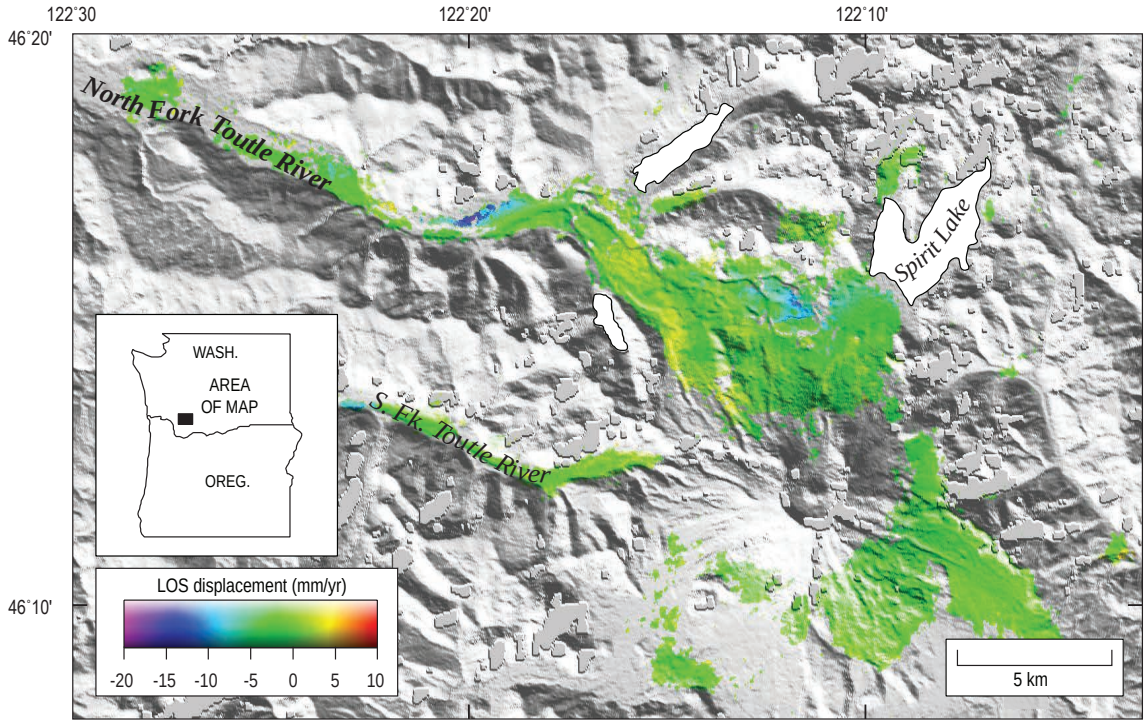

Figure 3. ERS-1/2, track 163, interferometric stack of Mount St. Helens, Washington, composed of seven interferograms spanning preeruptive 1993–2000 time period.

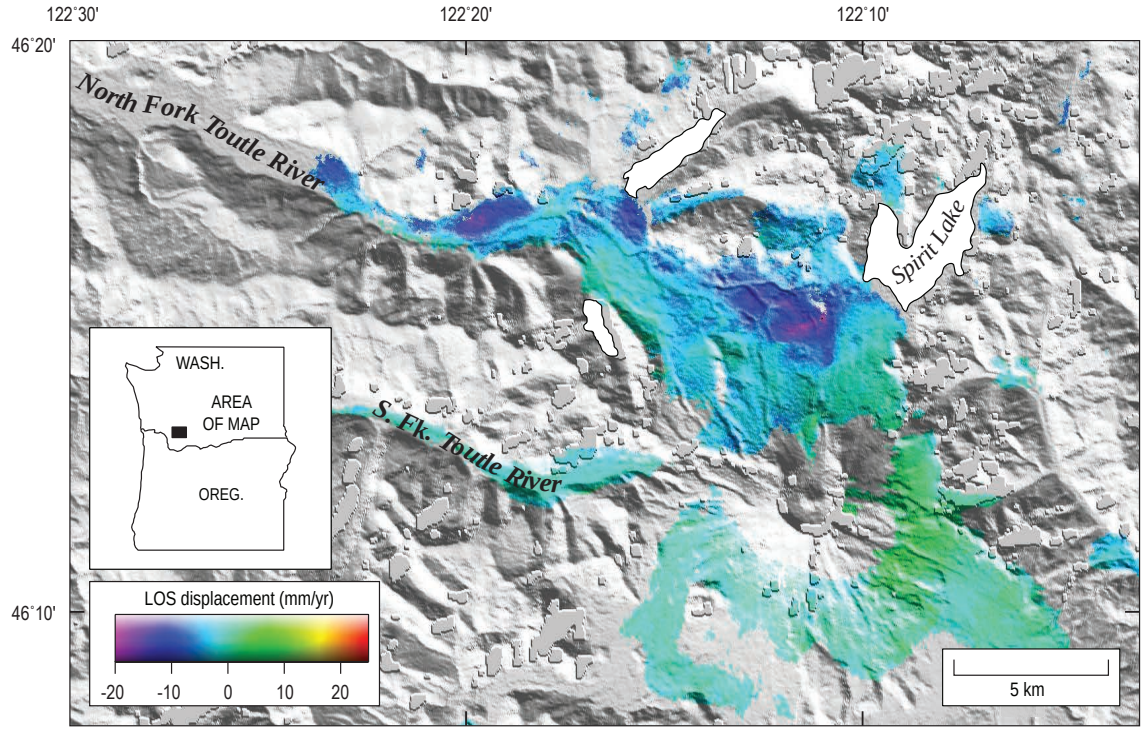

Figure 4. ERS-1/2, track 385, interferometric stack of Mount St. Helens, Washington, composed of 38 interferograms spanning preeruptive 1992–2001 time period.

slightly over the observation period, although the data are too noisy to be certain. Both regions, however, are apparent in coeruptive stacks that span 2004–5 (figs. 8–14), so neither area had ceased deforming by 2005.

Discussion

Lack of Preeruption Deformation

Dzurisin (2003) postulated that deep magma accumulation should precede volcanic unrest and eruption and might have gone undetected prior to the May 18, 1980, eruption of Mount St. Helens. He also suggested that InSAR is perhaps the best tool for detecting such deformation, as exemplified by discoveries of aseismic inflation at South Sister (Wicks and others, 2002) and Peulik (Lu and others, 2002b) volcanoes. Our results rule out surface displacements on the order of 1 cm or greater due to magma accumulation beneath Mount St. Helens between 1992 and late 2001 and between 2003 and the start of the 2004 eruption. It is unlikely that the period not covered by the InSAR stacks was the only time that displacements occurred; therefore, it is probable that no volcanowide

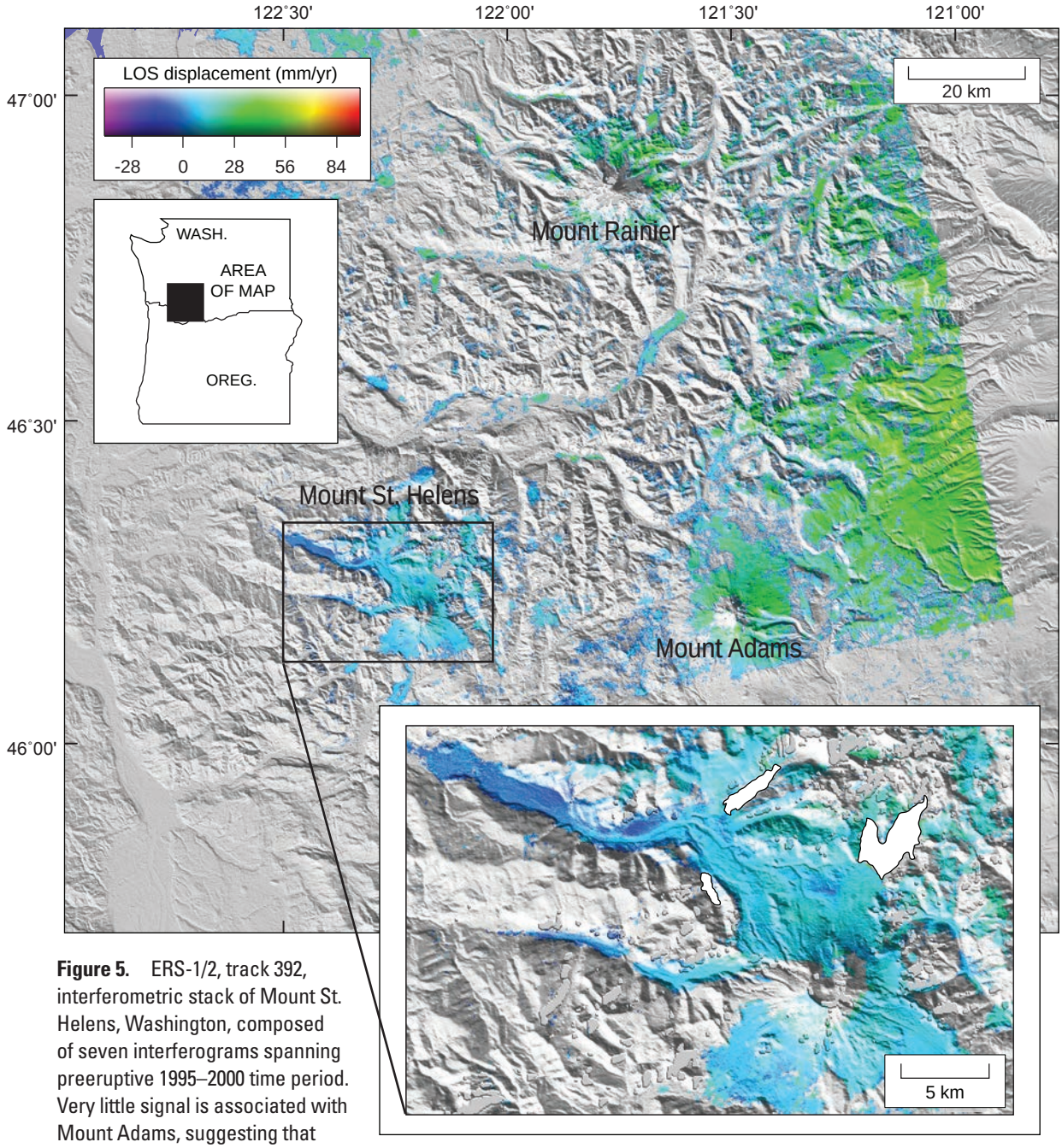

Figure 5. ERS-1/2, track 392, interferometric stack of Mount St. Helens, Washington, composed of seven interferograms spanning preeruptive 1995–2000 time period. Very little signal is associated with Mount Adams, suggesting that atmospheric artifacts are minimal.

displacements occurred during 1992–2004. How can this result be reconciled with Dzurisin's (2003) proposal?

Seismic and geodetic evidence from the late 1980s and early 1990s favor repressurization and possible resupply of the magma body located at about 6–10 km depth. Moran (1994) examined patterns of seismicity between 1987 and 1992 and concluded that the approximately 6- to 10-km-deep reservoir was being pressurized, probably by volatiles that exsolved during magma crystallization and were trapped beneath a seal in the shallow conduit. Seismicity, gas-emission events, and small explosions in 1989–91 may have been related to rupturing of this seal and escape of volatiles (Mastin, 1994). A seismic swarm in 1998 was accompanied by the emission of CO_2 (Gerlach and others, this volume, chap. 26), but whether this seismicity was related to magma migration or only the ascent of magmatic gases is unclear. Magma accumulation below 5.5 km depth is proposed by Musumeci and others (2002) to explain patterns of relocated seismicity. Lisowski and others (this volume, chap. 15) analyzed trilateration data collected in 1982 and 1991 and GPS data from 2000 and found evidence for areal dilatation between 1982 and 1991 that may indicate magma recharge. No significant changes were observed during the 1991–2000 time period. It is possible that magma was accumulating beneath Mount St. Helens only during the late 1980s and early 1990s and was manifested by deep seismicity, areal dilatation, and phreatic explosions (Mastin, 1994; Moran, 1994; Musumeci and others, 2002; Moran and others, this volume, chap. 2).

It seems that there is ample evidence for a pressure increase—either due to exsolution of volatiles, intrusion of new magma, or both—at ~6–10 km depth beneath Mount St. Helens in the years between the end of eruptive activity in 1986 and the start of the 2004 eruption. Changes in pressure or volume at this depth, if large enough, should result in displacements observable by InSAR because they would extend well outside the incoherent crater area without being overly broad or diffuse. The fact that no inflation was observed by InSAR during 1992–2004 (assuming that no deformation occurred during late 2001 to early 2003, when no InSAR data are available) suggests that either (1) the magnitude of volume increase (if magma accumulation occurred) or pressure increase (if only gas exsolution occurred) was insufficient to produce measurable surface displacements, (2) the increase in pressure or volume was accommodated by inelastic processes that did not deform the surface, or (3) the increase in pressure or volume occurred prior to 1992. Distinguishing among these mechanisms is not possible at present, although seismic and geodetic data (discussed above) that were collected after the end of the 1980–86 eruptive period and before InSAR results became available in 1992 favor option 3.

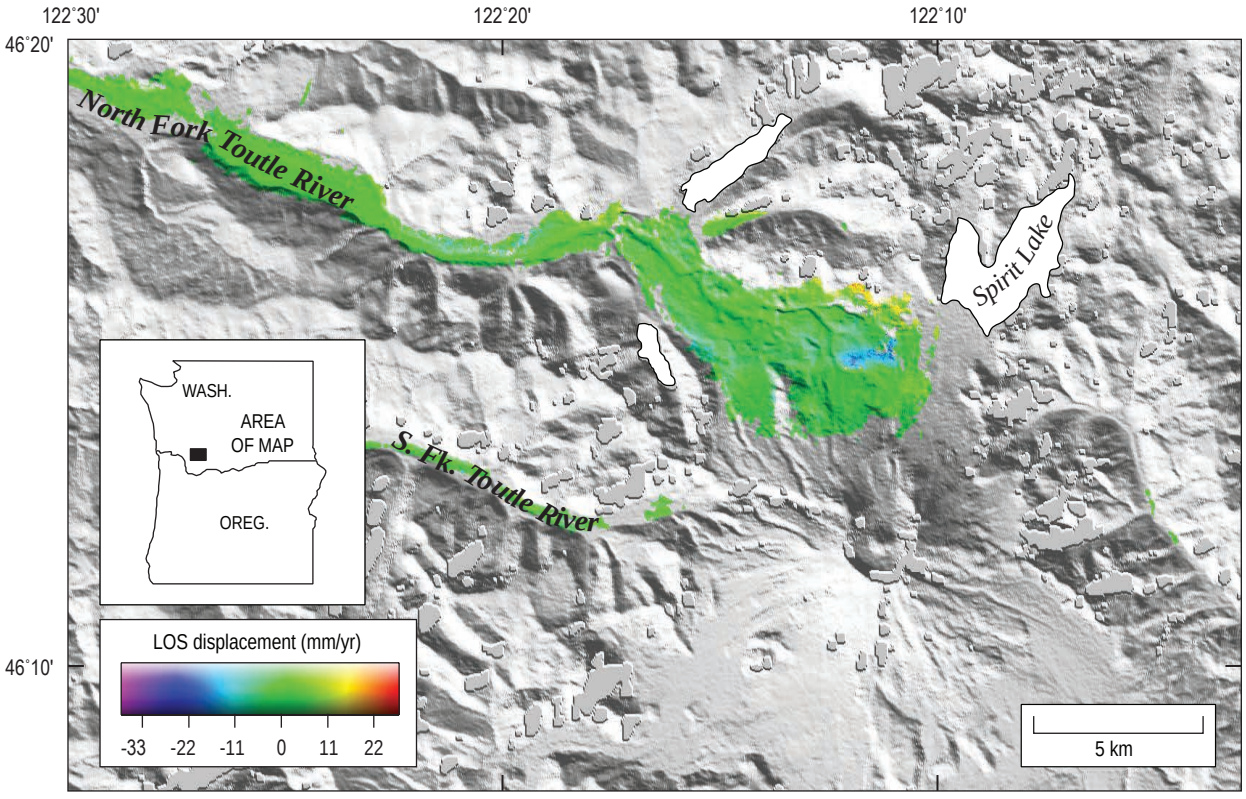

Figure 6. ENVISAT mode 2, track 156, interferometric stack of Mount St. Helens, Washington, composed of six interferograms spanning preeruptive 2003–2004 time period.

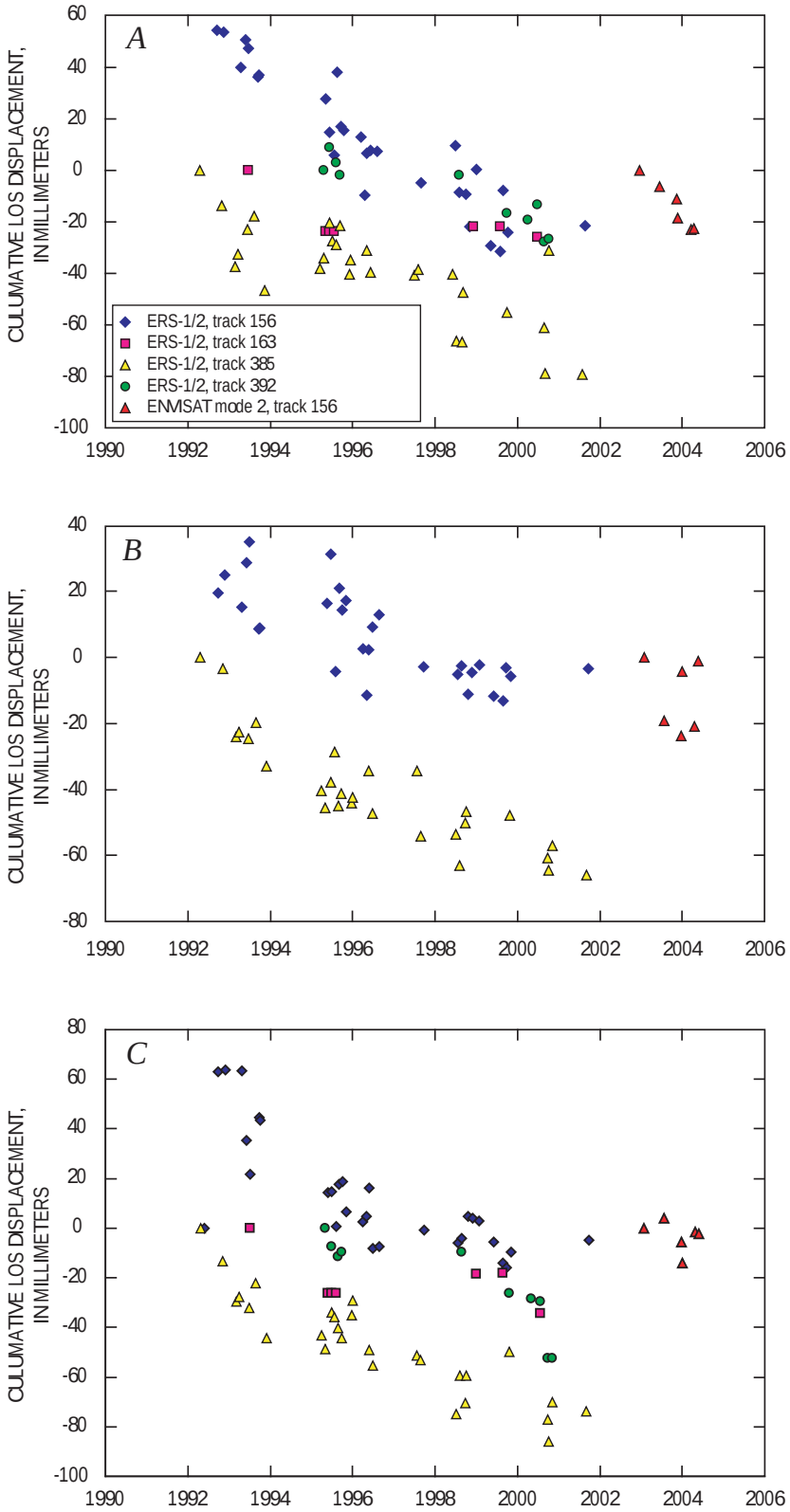

Figure 7. Time series showing line-of-sight (LOS) displacements of subsidence patches at (*A*) Johnston Ridge (site 1 in fig. 2), (*B*) Coldwater (site 2 in fig. 2), and (*C*) Elk Rock (site 3 in fig. 2). LOS displacements are relative to one another, so absolute value of Y axis is less important than changes in value over time. Note that more than 35 interferograms were used to generate time series for ERS tracks 156 and 385, whereas only 6–7 interferograms were used for ERS tracks 163 and 392, and ENVISAT track 156. Deformation rates determined from tracks with relatively few input interferograms could therefore be biased by atmospheric delay anomalies.

Subsidence Patches in the Debris-Avalanche Deposit

The origin of the localized subsidence patches on the debris-avalanche deposit is difficult to constrain and may be a result of several different processes. All three patches occur on the 1980 debris-avalanche deposit. Pyroclastic-flow deposits emplaced during explosive eruptions in 1980 bury the debris-avalanche unit at the base of Johnston Ridge near patch 1 but are not present at the other two patches (Rowley and others, 1981). The displacement patterns resemble poroelastic deformation caused by groundwater withdrawal (for example, Bawden and others, 2001), but there has been no deliberate removal of water from the debris-avalanche deposit. The subsidence has been occurring since at least 1992, and probably much longer, so subsidence mechanisms that occur on short time scales (days to months), including release of gas (Matthews and others, 2003), hydrocompaction due to rainfall (Hoblitt and others, 1985), and poroelastic deformation of the substrate (Lu and others, 2005a) cannot account for the longevity of the observed deformation and the lack of significant changes in subsidence rate over time (fig. 7). Instead, the deformation must be related to long-lived activity associated with the May 18, 1980, debris-avalanche deposit. Processes that have the potential to cause years-long subsidence of a loosely consolidated volcanic deposit like the Mount St. Helens debris-avalanche unit include cooling and contraction of an initially hot deposit (Masterlark and others, 2006), loading of a viscoelastic substrate (Briole and others, 1997; Stevens and others, 2001; Lu and others, 2005a; Masterlark and others, 2006), consolidation of a saturated or unusually dilated deposit (Major, 2000), and melting of buried ice (Branney and Gilbert, 1995; Everest and Bradwell, 2003).

The debris-avalanche deposit was emplaced onto a substrate of Tertiary volcanic rocks, with volcaniclastic sediments along river terraces of, and in, the upper part of the North Fork Toutle River valley and other drainages (Crandell, 1987; Evarts and others, 1987). The loosely consolidated debris-avalanche deposit has a volume of $2{,}500\times10^6$ m^3 and is composed mostly of cold dacite, andesite, and basalt, with probably less than 50×10^6 m^3 of the volume taken up by the hot (temperature greater than several hundred degrees Celsius) cryptodome that intruded the volcanic edifice in March–May 1980 (Voight and others, 1981; Glicken, 1996). The deposit reaches its maximum thickness, about 200 m, near the base of Johnston Ridge (but not at the exact location of the Johnston Ridge subsidence patch; Glicken, 1996). Glacial ice is thought to represent at least 100×10^6 m^3 of the volume of the unit (Brugman and Meier, 1981; Glicken, 1996). Much of this ice was buried by debris, and localized melting may have contributed to the formation of the North Fork Toutle River lahar on the afternoon of May 18, 1980 (Fairchild, 1987). Water derived from groundwater in the precollapse volcano and glacial ice incorporated into the debris avalanche amounted to approximately 250×10^6 m^3, about 12 percent of the total volume of the deposit (Glicken, 1996). A ground-water system developed in the unit following emplacement, as confirmed by numerous springs and seeps in the deposit, and seasonal changes in pond levels (J. Major, oral commun., 2006). Some parts of the debris-avalanche deposit were also saturated on emplacement, including two of the three patches of subsidence observed by InSAR (at the outlet of Coldwater Lake and below Elk Rock). The area below Elk Rock may have been the source of the May 18, 1980, North Fork Toutle River lahar (Fairchild, 1987; Glicken, 1996), and mud volcanoes caused by dewatering were observed near the outlet of Coldwater Lake in 1981 (J. Major, oral commun, 2006). In the weeks following May 18, 1980, Banks and Hoblitt (1996) measured the temperature of the deposit in shallow holes and found temperatures to be less than 100°C, with no increase in temperature below about 1.5 m. These data suggest that the maximum temperature of the deposit was no greater than boiling (Voight and others, 1981; Banks and Hoblitt, 1996), although temperatures probably varied widely depending on deposit composition (for example, shattered cryptodome versus cold volcanic edifice).

The initial emplacement temperature of the deposit would have to have been unreasonably high to cause subsidence due to cooling and contraction, as suggested by analogy with pyroclastic flows emplaced in 1986 at Augustine Volcano, Alaska. Masterlark and others (2006) used the known 3 cm/yr subsidence rate of Augustine's 1986 deposits (measured 13 years after the flows were emplaced) and the known maximum 126-m deposit thickness to model an initial temperature of 640°C. Decreasing the initial temperature to 500°C required a maximum pyroclastic-flow thickness of 336 m to produce the same subsidence rate. By analogy, the debris-avalanche deposit at Mount St. Helens would need to have an emplacement temperature of over 600°C to produce the subsidence observed by InSAR. Considering the small amount of hot cryptodome incorporated in the deposit and relatively low measured temperatures, it is unlikely that the temperature of significant volumes of the unit approached the required several hundred degrees.

Subsidence in response to a recently emplaced load occurs as the substrate relaxes viscoelastically beneath the load. The magnitude of the subsidence should be directly proportional to the size of the load and the thickness of the substrate (Briole and others, 1997). Subsidence patches on the Mount St. Helens debris-avalanche deposit, however, do not correlate with deposit thickness, although heterogeneity in pre-1980 surficial geology could still allow for subsidence due to loading. Loosely consolidated, relatively low-density sediment in and around the North Fork Toutle valley may be compacting under the load of the debris-avalanche deposit. Subsidence would occur only on parts of the debris-avalanche deposit that overlie accumulated sediment, explaining the patchiness of the subsidence and the fact that deformation occurs mostly where the unit lies near or above the buried channel and floodplains of the North Fork Toutle River. Testing this hypothesis is

difficult without additional knowledge of the thickness and extent of sedimentary deposits prior to the catastrophic debris avalanche of May 18, 1980.

Consolidation of granular deposits is a function of water content and diffusivity; compaction and subsidence occur in saturated deposits as water is removed (Major, 2000). Localized subsidence undoubtedly resulted as water seeped from saturated parts of the debris-avalanche deposit, and dewatering persisted through 2005 on the basis of springs and seeps found throughout the unit (J. Major, oral commun., 2006). Depending on the diffusivity and saturated thickness of the deposit, gravitational consolidation resulting from dewatering and diffusion of fluid pressure in excess of hydrostatic pressure could last for years, causing subsidence for decades after the deposit was emplaced (Major, 2000).

Melting of buried ice as a long-term subsidence mechanism could only occur if ice within the debris-avalanche deposit melted slowly over decades. In cold deposits (for example, the terminal moraine of a retreating glacier), buried ice can persist for hundreds of years (Everest and Bradwell, 2003). Could ice have survived more than 25 years buried in the Mount St. Helens debris-avalanche deposit? The answer depends on the deposit temperature and whether ice survived as large blocks or pulverized grains. If the entire deposit were initially about boiling (Banks and Hoblitt, 1996), there is little chance that even large blocks of ice (25–50 m in diameter) could have survived more than a few months after May 18, 1980 (Fairchild, 1987). Some parts of the debris-avalanche deposit were probably at ambient temperature, however, because much of the collapsed edifice, including most of the first landslide block, was composed of the cold outer skin of the volcano (including glacial ice; Glicken, 1996). Evidence for long-term survival of buried ice at Mount St. Helens is suggested by the discovery of subsurface ice during excavations near Spirit Lake by the U.S. Army Corps of Engineers almost 2 years after the May 18, 1980, eruption (Glicken, 1996). Slow melting of buried ice would account for the patchiness of the subsidence, as well as the lack of correlation between debris avalanche thickness and subsidence magnitude. There is, unfortunately, no way to know whether or not buried ice is the source of subsidence of the Mount St. Helens debris-avalanche deposit, but it remains a viable mechanism.

All of the possible subsidence mechanisms are asymptotic processes, meaning that subsidence rates of the debris-avalanche deposit patches should decay over time. No significant rate changes are apparent from the InSAR time series (fig. 7), so the mechanism of subsidence for the debris-avalanche deposit patches must be a long-term process, with changes in the rate of deformation requiring decades to manifest. Based on the temperature and composition of the debris-avalanche deposit and substrate, the observed patches of subsidence may be caused by differential compaction of sedimentary substrate along the buried North Fork Toutle River, gravitational consolidation of locally saturated or unusually dilated areas of the debris-avalanche deposit, or melting of buried ice. Using current knowledge, the relative contributions of these mechanisms cannot be determined; thus all three processes are viable causes for localized areas of subsidence on the May 18, 1980, debris-avalanche deposit.

Coeruptive stacks

Results

Unlike the preeruptive stacks, coeruptive stacks are inconsistent and heavily affected by atmospheric artifacts (figs. 8 through 14). The seven coeruptive stacks show all possible deformation patterns—no surface displacements, volcanowide inflation, and volcanowide deflation. Deflation of Mount St. Helens is suggested by ENVISAT mode 2, track 163 (fig. 9), ENVISAT mode 6, track 20 (fig. 12), and RADARSAT mode 2 (fig. 13). No deformation is apparent in the ENVISAT mode 2, track 156 (fig. 8), ENVISAT mode 2, track 385 (fig. 10), and ENVISAT mode 2, track 392 (fig. 11) stacks. Inflation, at least in two quadrants of the volcano, is indicated in the RADARSAT mode 5 (fig. 14) stack. These contradictory results can be reconciled by examining the character of the subsidence patch located at the base of Johnston Ridge, which was probably active during the coeruptive time period based on its persistence during the preeruptive interval and lack of decay over time (fig. 7*A*). This feature is only apparent in ENVISAT mode 2, track 163 (fig. 9), ENVISAT mode 6, track 20 (fig. 12), and the two RADARSAT beam modes (figs. 13 and 14). Stacks that do not show the subsidence patches are not sensitive to displacement rates of 2–3 cm/yr, on the same order as the expected volcanowide deflation signal measured by GPS (Lisowski and others, this volume, chap. 15).

The three interferograms that show volcanowide subsidence (figs. 9, 12, 13) are the stacks produced from at least nine input interferograms (table 1). We suspect that the averaged range changes in figures 8, 10, 11, and 14 are biased by atmospheric delay anomalies due to the limited number of interferograms used in the stacks. These stacks should not be considered for further analysis. Atmospheric delay artifacts in the stacks may also be recognized by topography-correlated fringes at presumably undeforming mountains also covered by the scenes (Beaudecel and others, 2000). Unfortunately, no mountains other than Mount St. Helens are coherent within, or covered by, the ENVISAT mode 2, track 163 (fig. 9) and ENVISAT mode 6, track 20 (fig. 12) stacks, and their quality cannot be assessed independently. Mount Adams, 60 km east of Mount St. Helens, has no associated phase-correlated topography in the RADARSAT mode 2 stack (fig. 13) which, together with the debris-avalanche subsidence patches also visible in that image, suggests that the stack is sensitive to deformation on the order of 1 cm/yr. As a result, the stack that is most representative of the coeruptive deformation state of Mount St. Helens is RADARSAT mode 2 (fig. 13). This stack suggests

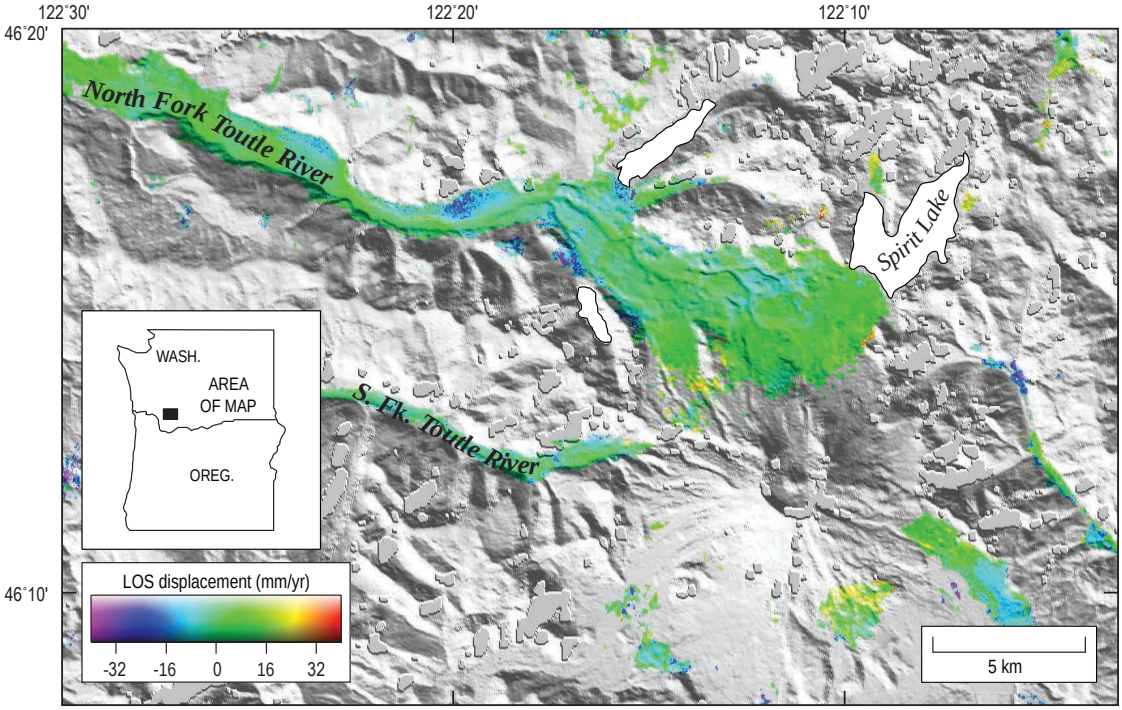

Figure 8. ENVISAT mode 2, track 156, interferometric stack of Mount St. Helens, Washington, composed of seven interferograms spanning coeruptive 2004–5 time period.

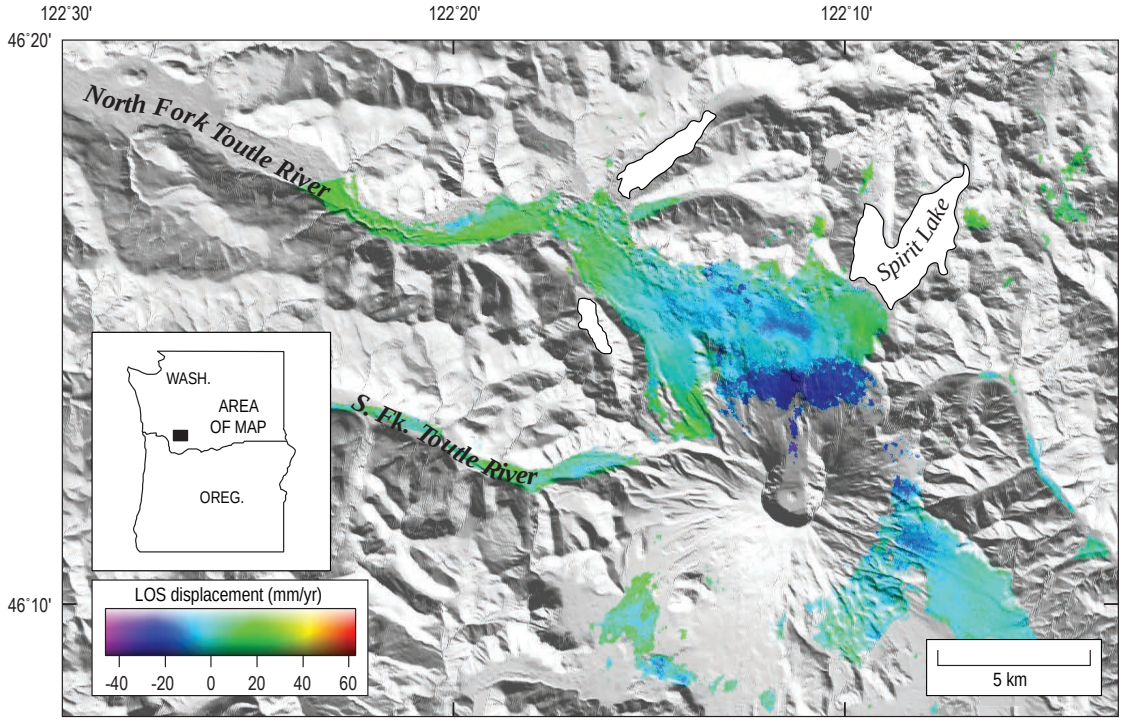

Figure 9. ENVISAT mode 2, track 163, interferometric stack of Mount St. Helens, Washington, composed of 13 interferograms spanning coeruptive 2004–5 time period.

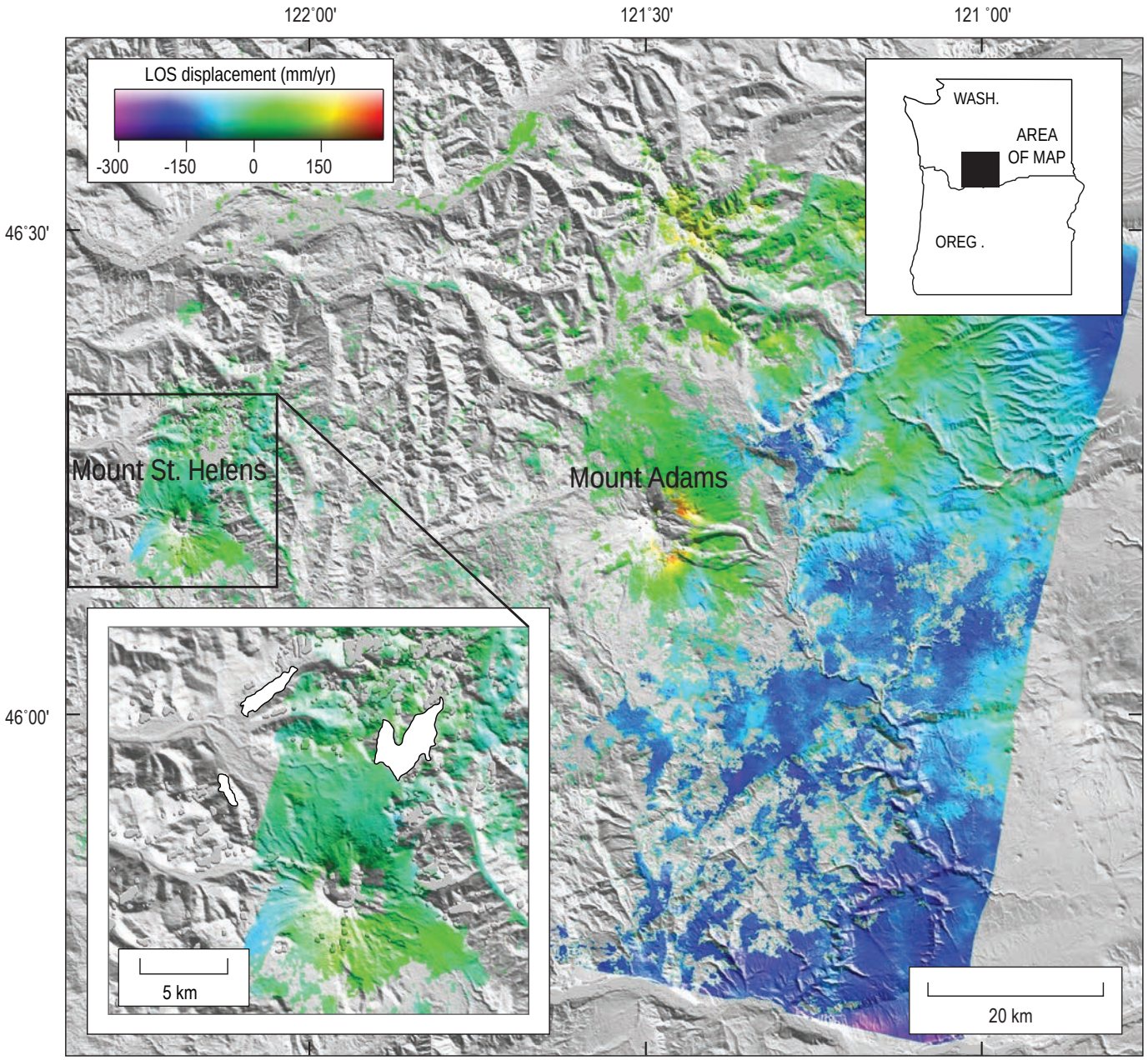

Figure 10. ENVISAT mode 2, track 385, interferometric stack of Mount St. Helens, Washington, composed of three interferograms spanning coeruptive 2004–5 time period. All three interferograms cover times of 70 days or fewer, so stacked phase has low signal-to-noise ratio and is characterized by phase that correlates with topography. This is especially apparent at Mount Adams.

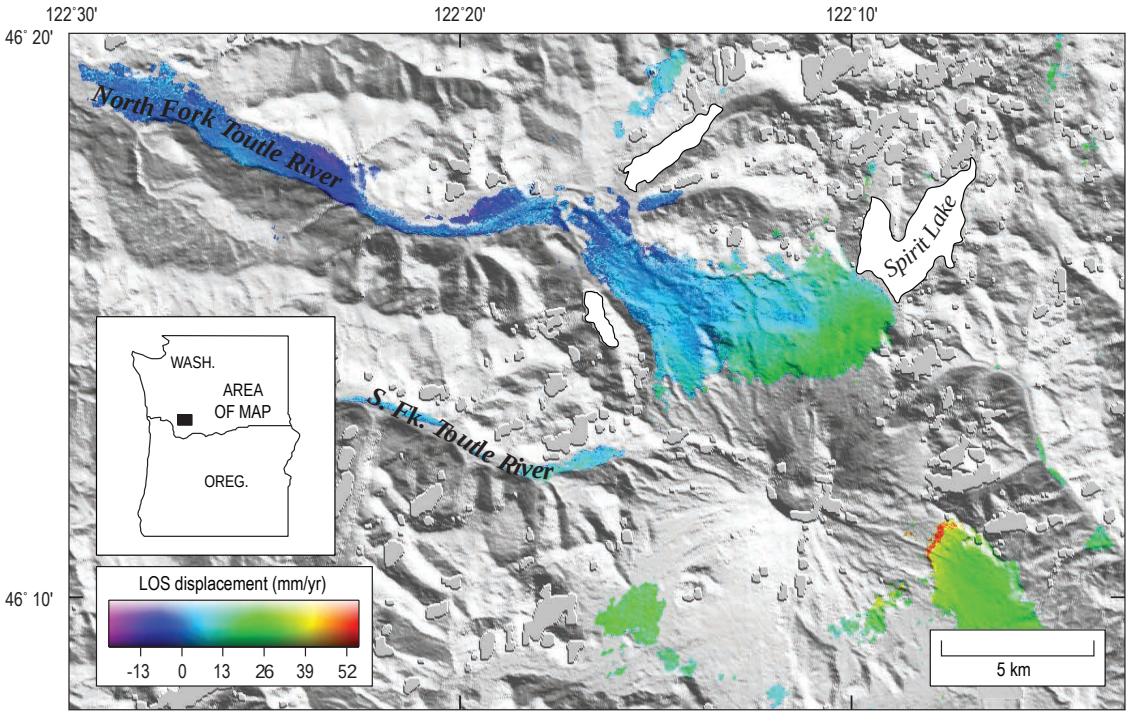

Figure 11. ENVISAT mode 2, track 392, interferometric stack of Mount St. Helens, Washington, composed of six interferograms spanning coeruptive 2004–5 time period.

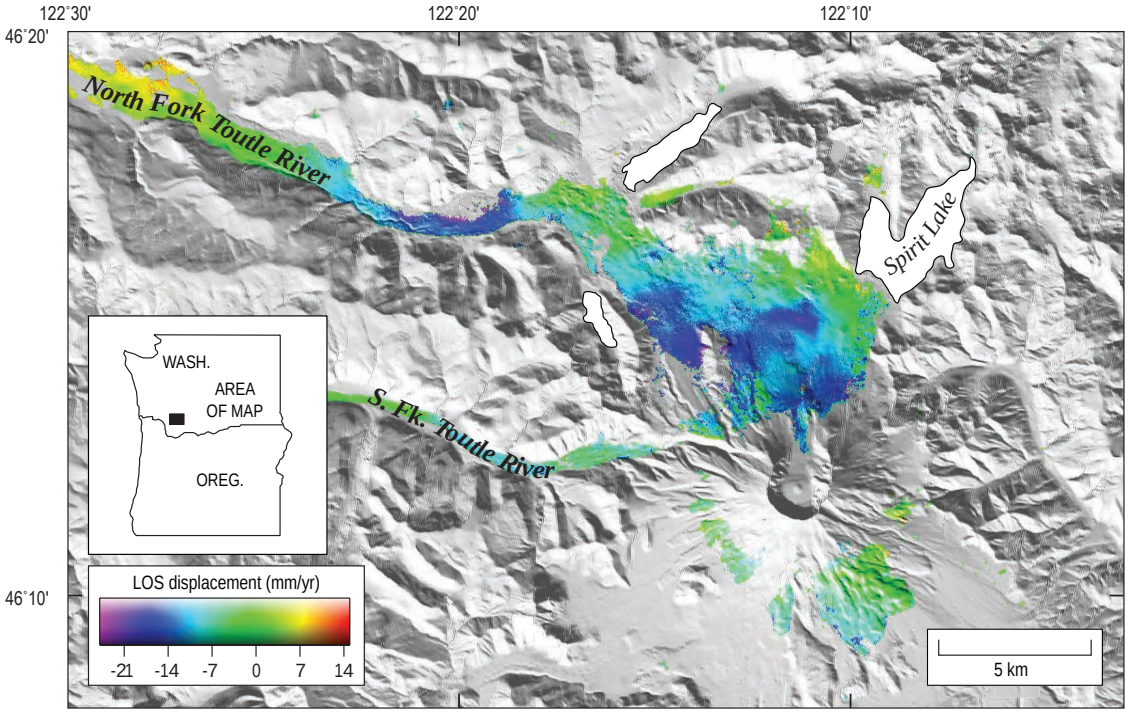

Figure 12. ENVISAT mode 6, track 20, interferometric stack of Mount St. Helens, Washington, composed of 13 interferograms spanning coeruptive 2004–5 time period.

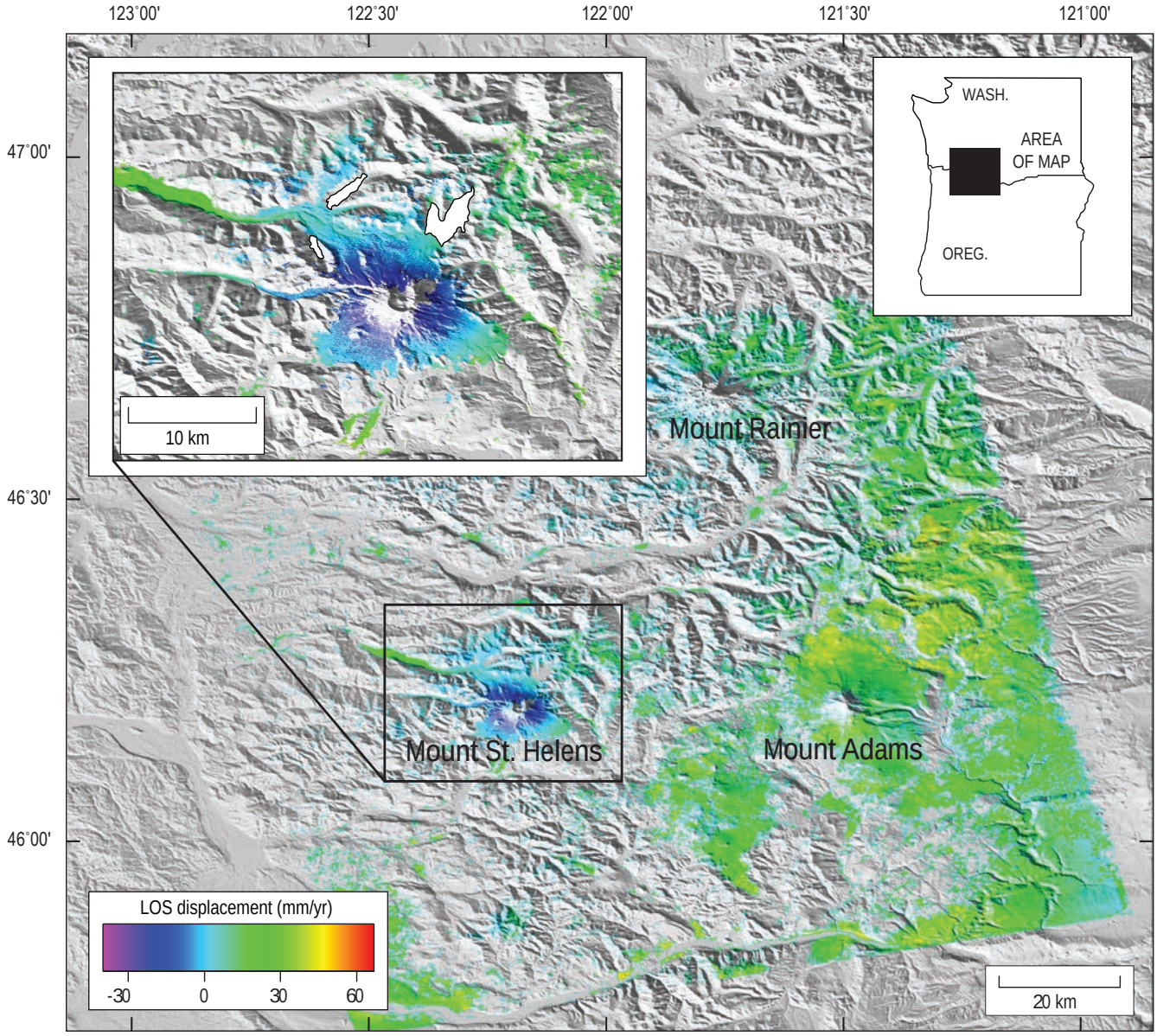

Figure 13. RADARSAT standard mode 2 ascending interferometric stack of Mount St. Helens, Washington, composed of nine interferograms spanning coeruptive 2004–5 time period. Stack clearly shows line-of-sight lengthening (subsidence) centered on Mount St. Helens which, as discussed in text, most likely reflects deformation of the ground surface. Atmospheric artifacts are probably minimized, as suggested by the lack of a significant signal associated with Mount Adams.

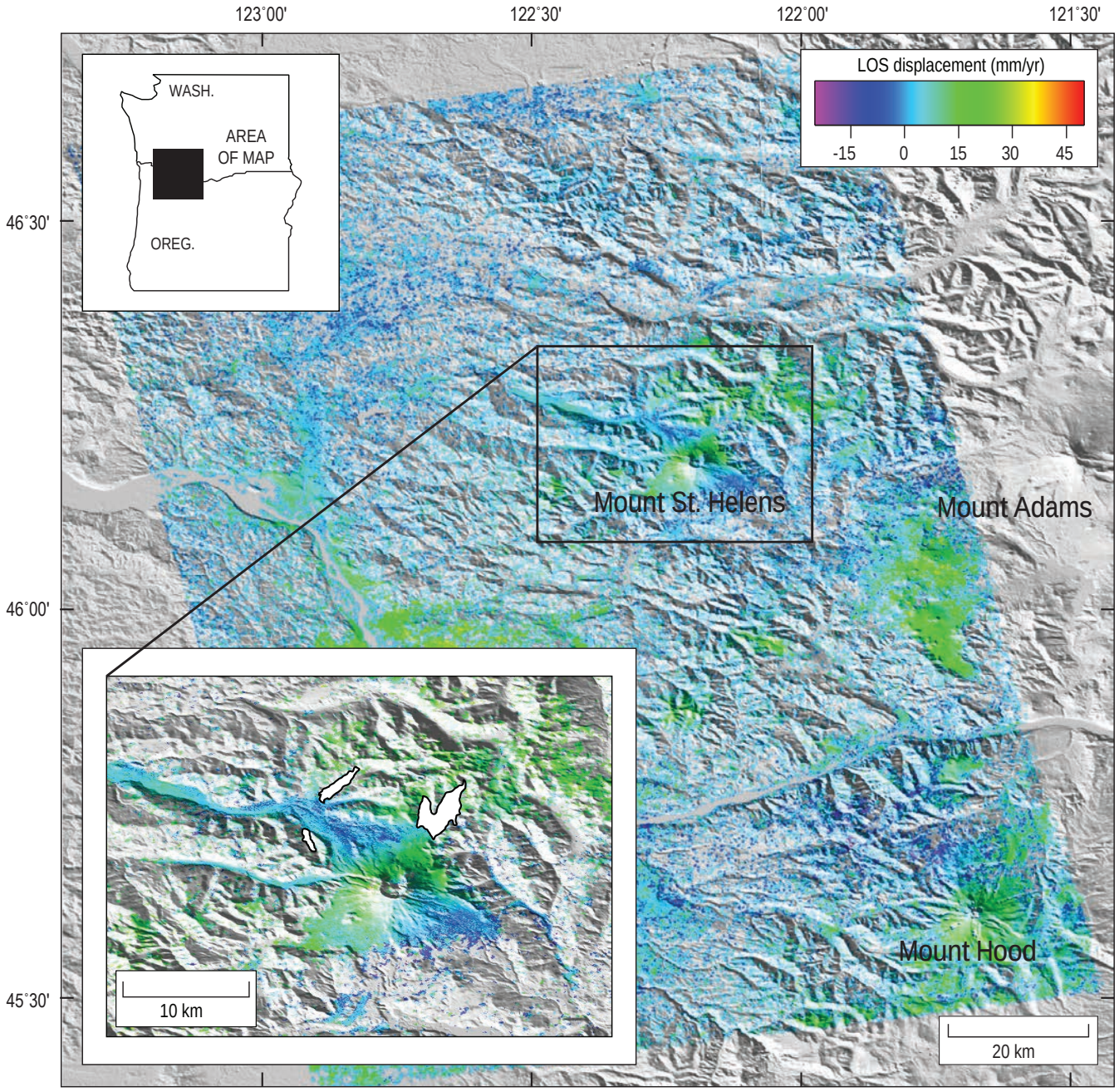

Figure 14. RADARSAT standard mode 5 ascending interferometric stack of Mount St. Helens, Washington, composed of six interferograms spanning coeruptive 2004–5 time period. Topography-correlated phase at Mount Hood suggests the presence of atmospheric artifacts in the stack.

LOS lengthening (subsidence) of at least 40–50 mm/yr centered on Mount St. Helens (the maximum is probably greater but not recoverable given the incoherence in the crater) and extends radially outwards beyond the flanks of the volcano.

Discussion

We modeled the RADARSAT mode 2 dataset (fig. 13) by inverting the LOS displacements for a buried point source of volume change (Mogi, 1958). Other types of sources (for example, an ellipsoid or circular crack) might yield a better fit to the data, but it is difficult to justify the use of more complicated source geometries in light of the limited coherence around Mount St. Helens, especially in the crater area where the deformation appears to reach a maximum. The best-fitting point source is located at a depth of 12 km directly beneath the crater of Mount St. Helens and has a volume loss of 27×10^6 m^3/yr (fig. 15). The depth compares favorably with a point source model based on GPS data (Lisowski and others, this volume, chap. 15), but it is deeper than more-complicated ellipsoidal source models (Lisowski and others, this volume, chap. 15; Mastin and others, this volume, chap. 22) and the 6–10-km-depth range for a proposed magma reservoir based on seismic data (Scandone and Malone, 1985; Barker and Malone, 1991; Moran, 1994; Musumeci and others, 2002). The greater InSAR-derived model depth is probably due to the lack of InSAR data in the crater area and the availability of only a single component of displacement from one interferometric stack.

We also modeled the data using a horizontal dislocation (Okada, 1985) constrained to uniform opening only, which approximates a sill. The best-fitting dislocation was located at a depth of 18 km, much deeper than the point source, but it had a similar volume change of about 30×10^6 m^3/yr. The difference in depths between the point source and dislocation models is unsurprising. A similar relation, for example, was found between point source and horizontal dislocation models of subsidence at Medicine Lake volcano, northern California (Dzurisin and others, 2002). The great variability in depths between the models is an indication of the strong dependence of model fits on model geometry (Delaney and McTigue, 1994). More data, especially from the crater region where displacement magnitudes are greatest, and varied look angles, which would provide additional components of displacement, are required to better constrain the geometry, volume change, and depth of the subsidence source, as well as model error estimates. Using only a single interferometric stack, results are unavoidably more ambiguous.

The modeled volume change is much smaller than the approximately 70×10^6 m^3 extruded over the first year of the eruption, as determined from analyses of digital elevation models (Schilling and others, this volume, chap. 8). Some of the difference may be explained by the fact that the stack averages the initially greater rates of subsidence and extrusion that occurred during the first few weeks of the eruption, but this is probably a minor effect. It is tempting to speculate that most of the discrepancy between modeled and extruded volumes is evidence for replenishment of the midcrustal magma reservoir by an even deeper source. Delaney and McTigue (1994), however, pointed out that the volume of injection should only equal the volume of eruption if the host rock is incompressible—clearly an unrealistic condition. They also demonstrated that modeled volume changes at depth are highly dependent on source geometry. In addition, our models assume a homogenous, isotropic, elastic rheology, which is almost certainly not the case beneath Mount St. Helens, where temperatures will be

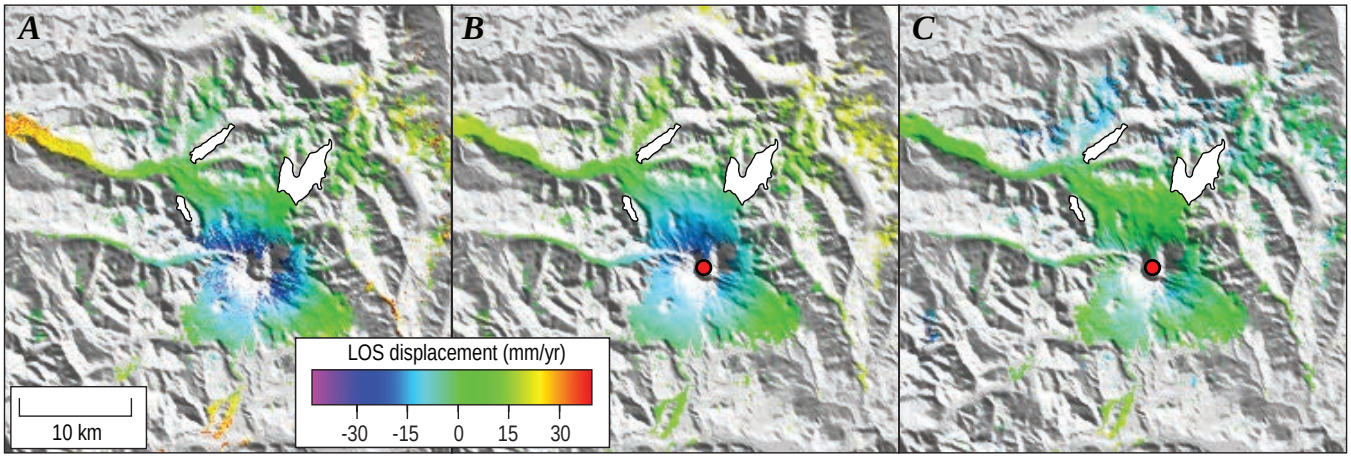

Figure 15. Observed (*A*), predicted (*B*), and residual (*C*) line-of-sight (LOS) displacements for RADARSAT standard mode 2 stack of Mount St. Helens, Washington (fig. 13), resulting from model that assumes point source of volume decrease (red circle) at depth of 12 km. LOS displacements scaled to maximize displacements around Mount St. Helens and differ from those in figure 13 for same interferogram.

elevated above the local geotherm due to the presence of the active magmatic system. Nonelastic rheologies can have a profound effect on the relation between surface deformation volume and source volume or pressure change (for example, Newman and others, 2001, 2006).

Nevertheless, it remains possible that the midcrustal magma reservoir was being replenished during the eruption, and that the discrepancy between modeled and extruded volumes was due to magma extrusion outpacing influx into the reservoir. Any surface inflation that might have resulted from recharge of the reservoir would have been masked by the greater deflation signal resulting from magma withdrawal and depressurization. Mastin and others (this volume, chap. 22) address this possibility in greater detail.

Conclusions

Interferograms from several independent tracks have been examined for signs of pre-and coeruptive deformation at Mount St. Helens. We can find no evidence for volcanowide displacements during time periods covered by stacks of radar interferograms (1992 to late 2001 and early 2003 until the onset of eruptive activity in September 2004). Seismic and geodetic evidence suggests repressurization, and possible resupply, of the 6- to 10-km-depth magma reservoir during the late 1980s and early 1990s, but this activity did not result in surface deformation detectable by InSAR during 1992–2004. We did find several small (1–2-km-diameter) patches of subsidence on the 1980 debris-avalanche deposit, one of which was recognized previously from individual interferograms of Mount St. Helens, and attribute this deformation to viscoelastic relaxation of loosely consolidated substrate under a load, differential consolidation of the deposit, or melting of ice buried within the deposit. Tracking the continued motion of these areas will serve as input for models of the post-depositional behavior of rapidly emplaced, unconsolidated deposits.

Coeruptive interferometric stacks are dominated by atmospheric noise, and only one of the seven stacks we assembled is demonstrably sensitive to deformation on the order of 1 cm or less. This stack indicates volcanowide deflation centered on the crater of Mount St. Helens and can be modeled by a point source of volume loss at a depth of 12 km beneath the edifice. This depth is at the lower boundary of a magma reservoir inferred from seismicity before 2004.

Both the pre- and coeruptive InSAR results have important implications for magma resupply, or lack thereof, before and during the 2004 eruption. Several papers in this volume address this question from differing perspectives and reach differing conclusions (for example, Moran and others, chap. 2; Dzurisin and others, chap. 14; Lisowski and others, chap. 15; Mastin and others, chap. 22; Gerlach and others, chap. 26; Pallister and others, chap. 30). Neither InSAR nor any other single data set can resolve the issue with certainty, but the weight of evidence seems to favor at least a minor amount of magma influx or pressurization of the midcrustal magma reservoir in the years before, and perhaps during, the eruption. The InSAR results, although not directly supportive of the idea, can be reconciled with it if the preeruption changes were small enough, accommodated by inelastic processes that did not measurably deform the surface, or occurred before 1992, and if the coeruption changes reflect a net deflation of the volcano due to extrusion outpacing recharge.

It is worth noting that, in general, the RADARSAT results are more coherent than those from ERS-1/2 and ENVISAT. A possible explanation for this discrepancy is that RADARSAT's H/H polarization provides better coherence in vegetated areas than V/V, which is the standard mode for ERS-1/2 and ENVISAT. Additional investigations into this possibility are warranted, as the result may suggest that one polarization mode is preferred over others for InSAR studies.

Our work has demonstrated the importance of including numerous interferograms in stacks. Coeruption stacks with less than nine input interferograms showed no signs of deflation that is known to be occurring from GPS. That our preeruption stacks span many more years and make use of many more interferograms than the coeruption stacks is the reason for the better signal-to-noise ratio in the preeruption stacks. The addition to the coeruptive stacks of InSAR data that extend through 2006 and beyond, assuming the eruption continues, will significantly reduce the magnitude of the atmospheric noise, allowing for more detailed analysis of surface deformation and associated source mechanisms.

Acknowledgments

Summer Miller provided invaluable assistance in preparing the ERS-1/2 and ENVISAT data sets for stacking. Paul Lundgren provided code for time series analysis, which Sarah Menassian modified for use with this project. Rick Hoblitt and Don Swanson offered much-needed guidance with respect to the emplacement of the Mount St. Helens debris avalanche, and discussions with Jon Major, Dick Iverson, and Joe Walder stimulated a closer look at the subsidence patches in the debris-avalanche deposit. Jon Major's advice concerning the behavior of saturated sedimentary deposits was especially valuable. Oh-Ig Kwoun assisted with processing RADARSAT data. We are indebted to Chuck Wicks, Daniel Dzurisin, and Seth Moran for thoughtful reviews and Jane Takahashi for thorough edits. Figures 1–6 and 8–15 were made using the Generic Mapping Tools (GMT) software (Wessel and Smith, 1998). ERS-1, ERS-2, and ENVISAT SAR data are copyrighted 1992–2005 by ESA and provided by Alaska Satellite Facility (ASF) and ESA Category-1 grants 2648 and 2765. RADARSAT-1 data are copyrighted by Canadian Space Agency and were provided by ASF. We thank the ASF for supporting RADARSAT-1 data acquisitions.

References Cited

Amelung, F., Jónsson, S., Zebker, H., and Segall, P., 2000a, Widespread uplift and 'trapdoor' faulting on Galápagos volcanoes observed with radar interferometry: Nature, v. 407, no. 6807. p. 993–996.

Amelung, F., Oppenheimer, C., Segall, P., and Zebker, H., 2000b, Ground deformation near Gada 'Ale Volcano, Afar, observed by radar interferometry: Geophysical Research Letters, v. 27, no. 19, p. 3093–3096.

Banks, N.G., and Hoblitt, R.P., 1996, Direct temperature studies of the Mount St. Helens deposits, 1980–1981: U.S. Geological Survey Professional Paper 1387, 76 p.

Barker, S.E., and Malone, S.D., 1991, Magmatic system geometry at Mount St. Helens modeled from the stress field associated with posteruptive earthquakes: Journal of Geophysical Research, v. 96, no. B7, p. 11883–11894.

Bawden, G.W., Thatcher, W., Stein, R.S., Hudnit, K.W., and Peltzer, G., 2001, Tectonic contraction across Los Angeles after removal of groundwater pumping effects: Nature, v. 412, no. 6849, p. 812–815.

Beaudecel, F., Briole, P., and Froger, J.-L., 2000, Volcano-wide fringes in ERS synthetic aperture radar interferograms of Etna (1992–1998); deformation or tropospheric effect?: Journal of Geophysical Research, v. 105, no. B7, p. 16391–16402.

Berardino, P., Fornaro, G., Lanari, R., and Sansosti, E., 2002, A new algorithm for surface deformation monitoring based on small baseline differential SAR interferograms: IEEE Transactions on Geoscience and Remote Sensing, v. 40, no. 11, p. 1–10.

Bevington, P.R., and Robinson, D.K., 1992, Data reduction and error analysis for the physical sciences (2d ed.): Boston, McGraw-Hill, 328 p.

Branney, M.J., and Gilbert, J.S., 1995, Ice-melt collapse pits and associated features in the 1991 lahar deposits of Volcán Hudson, Chile—criteria to distinguish eruption-induced glacier melt: Bulletin of Volcanology, v. 57, no. 5, p. 293–302.

Briole, P., Massonnet, D., and Delacourt, C., 1997, Post-eruptive deformation associated with the 1986–87 and 1989 lava flows of Etna detected by radar interferometry: Geophysical Research Letters, v. 24, no. 1, p. 37–40.

Brugman, M.M., and Meier, M.F., 1981, Response of glaciers to the eruptions of Mount St. Helens, *in* Lipman, P.W., and Mullineaux, D.R., eds., The 1980 eruptions of Mount St. Helens, Washington: U.S. Geological Survey Professional Paper 1250, p. 743–756.

Cashman, K.V., 1988, Crystallization of Mount St. Helens 1980–1986 dacite: a quantitative textural approach: Bulletin of Volcanology, v. 50, no. 3, p. 194–209.

Cashman, K.V., 1992, Groundmass crystallization of Mount St, Helens dacite, 1980–1986; a tool for interpreting shallow magmatic processes: Contributions to Mineralogy and Petrology, v. 109, no. 4, p. 431–449, doi:10.1007/BF00306547.

Chen, C.W., and Zebker, H.A., 2001, Two-dimensional phase unwrapping with use of statistical models for cost functions in nonlinear optimization: Journal of the Optical Society of America A, v. 18, no. 2, p. 338–351.

Crandell, D.R., 1987, Deposits of pre-1980 pyroclastic flows and lahars from Mount St. Helens volcano, Washington: U.S. Geological Survey Professional Paper 1444, 91 p.

Delaney, P.T., and McTigue, D.F., 1994, Volume of magma accumulation or withdrawal estimated from surface uplift or subsidence, with application to the 1960 collapse of Kilauea Volcano: Bulletin of Volcanology, v. 56, nos. 6–7, p. 417–424.

Diefenbach, A.K., and Poland, M.P., 2003, InSAR analysis of surface deformation at Mount St. Helens, Washington [abs.]: Geological Society of America Abstracts with Programs, v. 35, no. 6, p. 562.

Dzurisin, D., 2003, A comprehensive approach to monitoring volcano deformation as a window on the eruption cycle: Reviews of Geophysics, v. 41, no. 1, 29 p., doi:1010,1029/2001RG000107.

Dzurisin D., Poland, M.P., and Bürgmann, R., 2002, Steady subsidence of Medicine Lake volcano, northern California, revealed by repeated leveling surveys: Journal of Geophysical Research, v. 107, no. B12, doi:10.1029/2001JB000893.

Dzurisin, D., Lisowski, M., Wicks, C.W., Jr., Poland, M.P., and Endo, E.T., 2006, Geodetic observations and modeling of ongoing inflation at the Three Sisters volcanic center, central Oregon Cascade Range, USA: Journal of Volcanology and Geothermal Research, v. 150, nos. 1–3, p. 35–54.

Dzurisin, D., Lisowski, M., Poland, M.P., Sherrod, D.R., and LaHusen, R.G., 2008, Constraints and conundrums resulting from ground-deformation measurements made during the 2004–2005 dome-building eruption of Mount St. Helens, Washington, chap. 14 *of* Sherrod, D.R., Scott, W.E., and Stauffer, P.H., eds., A volcano rekindled; the renewed eruption of Mount St. Helens, 2004–2006: U.S. Geological Survey Professional Paper 1750 (this volume).

Evarts, R.C., Ashley, R.P., and Smith, J.G., 1987, Geology of the Mount St. Helens area: Record of discontinuous volcanic and plutonic activity in the Cascade arc of southern Washington: Journal of Geophysical Research, v. 92, no. B10, p. 10155–10169.

Everest, J., and Bradwell, T., 2003, Buried glacier ice in southern Iceland and its wider significance: Geomorphology, v. 52, nos. 3–4, p. 347–358

Farr, T.G., and Kobrick, M., 2000, Shuttle Radar Topography Mission produces a wealth of data: Eos (American Geophysical Union Transactions), v. 81, no. 48, p. 583, 585.

Fairchild, L.H., 1987, The importance of lahar initiation processes, *in* Costa, J.E., and Wieczorek, G.F., eds., Debris flows/avalanches—processes, recognition, and mitigation: Geological Society of America Reviews in Engineering Geology 7, p. 51–61.

Fialko, Y., and Simons, M., 2001, Evidence for on-going inflation of the Socorro magma body, New Mexico, from Interferometric Synthetic Aperture Radar imaging: Geophysical Research Letters, v. 28, no. 18, p. 3549–3552.

Gerlach, T.M., McGee, K.A., and Doukas, M.P., 2008, Emission rates of CO_2, SO_2, and H_2S, scrubbing, and preeruption excess volatiles at Mount St. Helens, 2004–2005, chap. 26 *of* Sherrod, D.R., Scott, W.E., and Stauffer, P.H., eds., A volcano rekindled; the renewed eruption of Mount St. Helens, 2004–2006: U.S. Geological Survey Professional Paper 1750 (this volume).

Glicken, H., 1996, Rockslide-debris avalanche of May 18, 1980, Mount St. Helens volcano, Washington: U.S. Geological Survey Open-File Report 96–677, 90 p.

Goldstein, R.M., and Werner, C.L., 1998, Radar interferogram filtering for geophysical applications: Geophysical Research Letters, v. 25, no. 21, p. 4035–4038.

Hoblitt, R.P., Reynolds, R.L., and Larson, E.E., 1985, Suitability of nonwelded pyroclastic-flow deposits for studies of magnetic secular variation—a test based on deposits emplaced at Mount St. Helens, Washington, in 1980: Geology, v. 13, no. 4, p. 242–245.

Hooper, A., Zebker, H., Segall, P., and Kampes, B., 2004, A new method for measuring deformation on volcanoes and other natural terrains using InSAR persistent scatterers: Geophysical Research Letters, v. 31, no. 23, doi:10.1029/2004GL021737.

LaHusen, R.G., Swinford, K.J., Logan, M., and Lisowski, M., 2008, Instrumentation in remote and dangerous settings; examples using data from GPS "spider" deployments during the 2004–2005 eruption of Mount St. Helens, Washington, chap. 16 *of* Sherrod, D.R., Scott, W.E., and Stauffer, P.H., eds., A volcano rekindled; the renewed eruption of Mount St. Helens, 2004–2006: U.S. Geological Survey Professional Paper 1750 (this volume).

Lees, J.M., 1992, The magma system of Mount St. Helens; nonlinear high-resolution P-wave tomography: Journal of Volcanology and Geothermal Research, v. 53, nos. 1–4, p. 103–116.

Lisowski, M., Dzurisin, D., Endo, E.T., Iwatsubo, E.Y., and Poland, M.P., 2003, New results from a proposed PBO Cascade Volcano cluster III; post-eruptive deformation of Mount St. Helens, Washington, from EDM and GPS [abs.]: Geological Society of America Abstracts with Programs, v. 35, no. 6, p. 562.

Lisowski, M., Dzurisin, D., Denlinger, R.P., and Iwatsubo, E.Y., 2008, Analysis of GPS-measured deformation associated with the 2004–2006 dome-building eruption of Mount St. Helens, Washington, chap. 15 *of* Sherrod, D.R., Scott, W.E., and Stauffer, P.H., eds., A volcano rekindled; the renewed eruption of Mount St. Helens, 2004–2006: U.S. Geological Survey Professional Paper 1750 (this volume).

Lu, Z., Wicks, C.W., Jr., Power, J.A., and Dzurisin, D., 2000, Ground deformation associated with the March 1996 earthquake swarm at Akutan volcano, Alaska, revealed by satellite radar interferometry: Journal of Geophysical Research, v. 105, no. B9, p. 21483–21495.

Lu, Z., Power, J.A., McConnell, V.S., Wicks, C.W., Jr., and Dzurisin, D., 2002a, Preeruptive inflation and surface interferometric coherence characteristics revealed by satellite radar interferometry at Makushin Volcano, Alaska, 1993–2000: Journal of Geophysical Research, v. 107, no. B11, doi:10.1029/2001JB000970.

Lu, Z., Wicks, C.W., Jr., Dzurisin, D., Power, J.A., Moran, S.C., and Thatcher, W., 2002b, Magmatic inflation at a dormant stratovolcano; 1996–1998 activity at Mount Peulik volcano, Alaska, revealed by satellite radar interferometry: Journal of Geophysical Research, v. 107, no. B7, doi:10.1029/2001JB000471.

Lu, Z., Masterlark, T., Dzurisin, D., Rykhus, R., and Wicks, C.W., Jr., 2003a, Magma supply dynamics at Westdahl volcano, Alaska, modeled from satellite radar interferometry: Journal of Geophysical Research, v. 108, no. B7, 17 p., doi:10.1029/2002JB002311.

Lu, Z., Wicks, C.W., Jr., Dzurisin, D., Power, J., Thatcher, W., and Masterlark, T., 2003b, Interferometric Synthetic Aperture Radar studies of Alaska volcanoes: Earth Observation Magazine, v. 12, no. 3, p. 8–18.

Lu, Z., Masterlark, T., and Dzurisin, D., 2005a, Interferometric Synthetic Aperture Radar (InSAR) study of Okmok Volcano, Alaska, 1992–2003; magma supply dynamics and post-emplacement lava flow deformation: Journal of Geophysical Research, v. 110, no. B2, doi:10.01029/02004JB003148.

Lu, Z., Wicks, C.W., Jr., Kwoun, O.-I., Power, J.A., and Dzurisin, D., 2005b, Surface deformation associated with the March 1996 earthquake swarm at Akutan Island, Alaska, revealed by C-band ERS and L-band JERS radar interferometry: Canadian Journal of Remote Sensing, v. 31, no. 1, p. 7–20.

Lundgren, P., Casu, F., Manzo, M., Pepe, A., Berardino, P., Sansosti, E., and Lanari, R., 2004, Gravity and magma-induced spreading of Mount Etna Volcano revealed by satellite radar interferometry: Geophysical Research Letters, v. 31, no. 4, doi:10.01029/02003GL018736.

Major, J.J., 2000, Gravity-driven consolidation of granular slurries—implications for debris-flow deposition and deposit characteristics: Journal of Sedimentary Research, v. 70, no. 1, p. 64–83.

Masterlark, T., and Lu, Z., 2004, Transient volcano deformation sources imaged with interferometric synthetic aperture radar—application to Seguam Island, Alaska: Journal of Geophysical Research, v. 109, no. B1, doi:10.1029/2003JB002568.

Masterlark, T., Lu, Z., and Rykhus, R., 2006, Thickness distribution of a cooling pyroclastic flow deposit on Augustine Volcano, Alaska—optimization using InSAR, FEMs, and an adaptive mesh algorithm: Journal of Volcanology and Geothermal Research, v. 150, nos. 1–3, p. 186–201.

Mastin, L.G., 1994, Explosive tephra emissions at Mount St. Helens, 1989–1991; the violent escape of magmatic gas following storms?: Geological Society of America Bulletin, v. 106, no. 2, p. 175–185.

Mastin, L.G., Roeloffs, E., Beeler, N.M., and Quick, J.E., 2008, Constraints on the size, overpressure, and volatile content of the Mount St. Helens magma system from geodetic and dome-growth measurements during the 2004–2006+ eruption, chap. 22 *of* Sherrod, D.R., Scott, W.E., and Stauffer, P.H., eds., A volcano rekindled; the renewed eruption of Mount St. Helens, 2004–2006: U.S. Geological Survey Professional Paper 1750 (this volume).

Matthews, J.P., Kamata, H., Okuyama, S., Yusa, Y., and Shimizu, H., 2003, Surface height adjustments in pyroclastic-flow deposits observed at Unzen volcano by JERS-1 SAR interferometry: Journal of Volcanology and Geothermal Research, v. 125, nos. 3–4, p. 247–270.

Mogi, K., 1958, Relations between the eruptions of various volcanoes and the deformations of the ground surfaces around them: Bulletin of the Earthquake Research Institute, v. 36, no. 2, p. 99–134.

Moran, S.C., 1994, Seismicity at Mount St. Helens, 1987–1992: Evidence for repressurization of an active magmatic system: Journal of Geophysical Research, v. 99, no. B3, p. 4341–4354.

Moran, S.C., Kwoun, O.-I., Masterlark, T., and Lu, Z., 2006, On the absence of InSAR-detected volcano deformation spanning the 1995–1996 and 1999 eruptions of Shishaldin Volcano, Alaska: Journal of Volcanology and Geothermal Research, v. 150, nos. 1–3, p. 119–131.

Moran, S.C., Malone, S.D., Qamar, A.I., Thelen, W.A., Wright, A.K., and Caplan-Auerbach, J., 2008, Seismicity associated with renewed dome building at Mount St. Helens, 2004–2005, chap. 2 *of* Sherrod, D.R., Scott, W.E., and Stauffer, P.H., eds., A volcano rekindled; the renewed eruption of Mount St. Helens, 2004–2006: U.S. Geological Survey Professional Paper 1750 (this volume).

Musumeci, C., Gresta, S., and Malone, S.D., 2002, Magma system recharge of Mount St. Helens from precise relative hypocenter location of microearthquakes: Journal of Geophysical Research, v. 107, no. B10, 2264, p. ESE 16-1–ESE 16-9, doi:10.1029/2001JB000629.

Newman, A.V., Dixon, T.H., Ofoegbu, G.I., and Dixon, J.E., 2001, Geodetic and seismic constraints on recent activity at Long Valley Caldera, California; evidence for viscoelastic rheology: Journal of Volcanology and Geothermal Research, v. 105, no. 3, p. 183–206.

Newman, A.V., Dixon, T.H., and Gourmelen, N., 2006, A four-dimensional viscoelastic deformation model for Long Valley caldera, California, between 1995 and 2000: Journal of Volcanology and Geothermal Research, v. 150, nos. 1–3, p. 244–269.

Okada, Y., 1985, Surface deformation due to shear and tensile faults in a half-space: Bulletin of the Seismological Society of America, v. 75, no. 4, p. 1135–1154.

Pallister, J.S., Hoblitt, R.P., Crandell, D.R., and Mullineaux, D.R., 1992, Mount St. Helens a decade after the 1980 eruptions; magmatic models, chemical cycles, and a revised hazards assessment: Bulletin of Volcanology, v. 54, no. 2, p. 126–146, doi: 10.1007/BF00278003.

Pallister, J.S., Thornber, C.R., Cashman, K.V., Clynne, M.A., Lowers, H.A., Mandeville, C.W., Brownfield, I.K., and Meeker, G.P., 2008, Petrology of the 2004–2006 Mount St. Helens lava dome—implications for magmatic plumbing and eruption triggering, chap. 30 *of* Sherrod, D.R., Scott, W.E., and Stauffer, P.H., eds., A volcano rekindled; the renewed eruption of Mount St. Helens, 2004–2006: U.S. Geological Survey Professional Paper 1750 (this volume).

Peltzer, G., Crampé, F., Hensley, S., and Rosen, P., 2001, Transient strain accumulation and fault interaction in the Eastern California shear zone: Geology, v. 29, no. 11, p. 975–978.

Pritchard, M.E., and Simons, M., 2002, A satellite geodetic survey of large-scale deformation of volcanic centres in the central Andes: Nature, v. 418, no. 6894, p. 167–171.

Pritchard, M.E., and Simons, M., 2004a, An InSAR-based survey of volcanic deformation in the central Andes: Geochemistry, Geophysics, Geosystems, v. 5, no. 2, doi:02010.01029/02003GC000610.

Pritchard, M.E., and Simons, M., 2004b, An InSAR-based survey of volcanic deformation in the southern Andes: Geophysical Research Letters, v. 31, no. 15, doi:10.1029/2004GL020545.

Rowley, P.D., Kuntz, M.A., and MacLeod, N.S., 1981, Pyroclastic-flow deposits, *in* Lipman, P.W., and Mullineaux, D.R., eds., The 1980 eruptions of Mount St. Helens, Washington: U.S. Geological Survey Professional Paper 1250, p. 489–512.

Rutherford, M.J., Sigurdsson, H., Carey, S., and Davis, A., 1985, The May 18, 1980, eruption of Mount St. Helens—1. Melt composition and experimental phase equilibria: Journal of Geophysical Research, v. 90, no. B4, p. 2929–2947.

Scandone, R., and Malone, S.D., 1985, Magma supply, magma discharge and readjustment of the feeding system of Mount St. Helens during 1980: Journal of Volcanology and Geothermal Research, v. 23, nos. 3–4, p. 239–262, doi:10.1016/0377-0273(85)90036-8.

Schilling, S.P., Carrara, P.E., Thompson, R.A., and Iwatsubo, E.Y., 2004, Posteruption glacier development within the crater of Mount St. Helens, Washington, USA: Quaternary Research, v. 61, no. 3, p. 325–329.

Schilling, S.P., Thompson, R.A., Messerich, J.A., and Iwatsubo, E.Y., 2008, Use of digital aerophotogrammetry to determine rates of lava dome growth, Mount St. Helens, Washington, 2004–2005, chap. 8 *of* Sherrod, D.R., Scott, W.E., and Stauffer, P.H., eds., A volcano rekindled; the renewed eruption of Mount St. Helens, 2004–2006: U.S. Geological Survey Professional Paper 1750 (this volume).

Stevens, N.F., Wadge, G., Williams, C.A., Morley, J.G., Muller, J.-P., Murray, J.B., and Upton, M., 2001, Surface movements of emplaced lava flows measured by synthetic aperture radar interferometry: Journal of Geophysical Research, v. 106, no. B6, p. 11293–11313.

Voight, B., Glicken, H., Janda, R.J., and Douglass, P.M., 1981, Catastrophic rockslide avalanche of May 18, *in* Lipman, P.W., and Mullineaux, D.R., eds., The 1980 eruptions of Mount St. Helens, Washington: U.S. Geological Survey Professional Paper 1250, p. 347–377.

Wadge, G., Mattioli, G.S., and Herd, R.A., 2006, Ground deformation at Soufrière Hills Volcano, Montserrat during 1998–2000 measured by radar interferometry and GPS: Journal of Volcanology and Geothermal Research, v. 152, nos. 1–2, p. 157–173.

Walder, J.S., Schilling, S.P., Vallance, J.W., and LaHusen, R.G., 2008, Effects of lava-dome growth on the Crater Glacier of Mount St. Helens, Washington, chap. 13 *of* Sherrod, D.R., Scott, W.E., and Stauffer, P.H., eds., A volcano rekindled; the renewed eruption of Mount St. Helens, 2004–2006: U.S. Geological Survey Professional Paper 1750 (this volume).

Wessel, P., and Smith, W.H.F., 1998, New, improved version of Generic Mapping Tools released [abs.]: Eos (American Geophysical Union Transactions), v. 79, no. 47, p. 579.

Wicks, C.W., Jr., Thatcher, W., and Dzurisin, D., 1998, Migration of fluids beneath Yellowstone Caldera inferred from satellite radar interferometry: Science, v. 282, no. 5388, p. 458–462.

Wicks, C.W., Jr., Dzurisin, D., Ingebritsen, S., Thatcher, W., Lu, Z., and Iverson, J., 2002, Magmatic activity beneath the quiescent Three Sisters volcanic center, central Oregon Cascade Range, USA: Geophysical Research Letters, v. 29, no. 7, doi:10.1029/2001GL014205.

Wicks, C.W., Thatcher, W., Dzurisin, D., and Svarc, J., 2006, Uplift, thermal unrest, and magma intrusion at Yellowstone caldera: Nature, v. 440, no. 7080, p. 72–75, doi:10.1038/nature04507.

Wright, T., Parsons, B., and Fielding, E., 2001, Measurement of interseismic strain accumulation across the North Anatolian Fault by satellite radar interferometry: Geophysical Research Letters, v. 28, no. 10, p. 2117–2120.

Wright, T.J., Parsons, B., England, P.C., and Fielding, E.J., 2004, InSAR observations of low slip rates on the major faults of western Tibet: Science, v. 305, no. 5681, p. 236–239.

Zebker, H.A., Amelung, F., and Jonsson, S., 2000, Remote sensing of volcano surface and internal processes using radar interferometry, *in* Mouginis-Mark, P.J., Crisp, J.A., and Fink, J.H., eds., Remote sensing of active volcanism: Washington, D.C., American Geophysical Union Geophysical Monograph 116, p. 179–205.